Keck Adaptive Optics Note 455

Keck Next Generation Adaptive Optics Science Case Requirements Document

Release 1

Version 10
March 20, 2007

Keck Adaptive Optics Note 455

Keck Next Generation Adaptive Optics Science Case Requirements Document
Release 1

1 Introduction

1.1 Background

The Science Team of the Keck NGAO project is charged with 1) identifying the science requirements for the Next-Generation Adaptive Optics (NGAO) system, and 2) when design trade-offs must be made, ensuring that the NGAO system will be built with capabilities that enable key science cases to the greatest extent possible.

This document, which will be referred to as the Science Case Requirements Document (SCRD), is a "living document", and will be updated as the science case is developed with increasing fidelity. Initially, the SCRD will rely on and heavily reference the science cases developed for the Proposal to the Keck Science Steering Committee prepared in June 2006. Key issues are (a) the importance of the science enabled by the AO system and its accompanying instruments; (b) the advances offered by NGAO relative to AO systems being developed on other telescopes (discovery space); and (c) complementarity to the James Webb Space Telescope (JWST) and the Atacama Large Millimeter Array (ALMA), which will be commissioned on the same timescale as Keck NGAO.

Since June 2006, the Project Scientist has met with subgroups of the Science Team in order to re-examine the science cases, to develop more solid requirements, and to look in more detail at the associated Instrument and Observatory requirements. This document, Release 1 of the SCRD, describes AO and instrument requirements for a subset of NGAO science that is anticipated to have impact on the following AO system error budgets and instrument requirements:

- AO and instrument background requirements
- wavefront error
- astrometric error budget
- field of view and field of regard
- spectral resolution and multiplicity for the deployable integral field unit instrument
- AO capabilities at visible wavelengths

1.2 JWST Capabilities

The James Webb Space Telescope (JWST) is a cryogenic 6.5-m space telescope that is currently scheduled to be launched in 2013. It will have considerably higher faint-source sensitivity than Keck NGAO due to its low backgrounds. Its NIRCAM instrument will image in 14 filters in the 0.6-2.3 μm wavelength range that overlaps with Keck NGAO. NIRCAM will have a 2.2 x 2.2 arc-minute field of view, a pixel scale of 0.035 arc sec for 0.6-2.3 μm wavelengths, and coronagraphic capability. NIRCAM has diffraction-limited imaging for wavelengths between 2.4 and 5 μm, but not below 2 μm due both to the primary mirror quality specification and to the undersampled pixel scale (0.035 arcsec) within NIRCAM. Thus there is an interesting part of parameter space in which Keck NGAO can complement

JWST's imaging capabilities: diffraction limited imaging at wavelengths below 2 μm, over a field of order 2 arc-minutes on a side.

NIRSpec is a near infrared multi-object spectrograph for JWST in the 0.6 - 5 μm band. The primary goal for NIRSpec is enabling large surveys of faint galaxies (1<z<5) and determining their metallicity, star formation rate, and reddening. The NIRSpec design provides three observing modes: a low resolution R=100 prism mode, an R=1000 multi-object mode, and an R=2700 mode. In the R=100 and R=1000 modes NIRSpec provides the ability to obtain simultaneous spectra of more than 100 objects in the 3.4 x 3.5 arcmin field of view. Spatial pixel size will be 0.1 arc sec. There will be an integral field spectrograph with field of view 3" x 3", using 0.1 arc sec pixels, and a spectral resolution of R=2700.
Areas of parameter space in which Keck NGAO could complement JWST's spectroscopic capabilities include the following: 1) Spectroscopy (either slit or IFU) with spatial resolution better than 0.1 arc sec; 2) multi-IFU spectroscopy; 3) spectroscopy (slit or IFU) near the Keck diffraction limit at wavelengths 0.6 - 2 μm. It would be very difficult for Keck NGAO to compete with JWST at wavelengths longer than K band, because JWST will have far lower backgrounds. Even at the long-wavelength end of K band where the thermal background is important, NGAO will have difficulty competing in sensitivity with JWST's NIRSpec.

1.3 ALMA Capabilities

ALMA is a powerful new facility for mm and sub-mm astrophysics that is currently scheduled to begin science operations in 2012. It will consist of 54 12-m and 12 7-m antennas located at an altitude of 5000m (16,500 feet) in the Atacama desert of Chile. ALMA will observe, with very high sensitivity and resolution, the cold regions of the Universe which are optically dark, yet shine brightly in the millimeter portion of the electromagnetic spectrum. With baselines ranging from 150 m to 18 km, it will have spatial resolution down to 0.01 arc-seconds (0.004 arc-seconds at the highest frequencies), with typical resolution of 0.1 arc-second or better. It is expected to operate within atmospheric windows from 0.35 to 9 mm.

The design of the ALMA is being driven by three key science goals:

1. The ability to detect spectral line emission from CO or CII in a normal galaxy like the Milky Way at a redshift of z = 3, in less than 24 hours of observation.

2. The ability to image the gas kinematics in protostars and in protoplanetary disks around young Sun-like stars at a distance of 150 pc (roughly the distance of the star-forming clouds in Ophiuchus or Corona Australis), enabling the study of their physical, chemical and magnetic field structures and to detect the tidal gaps created by planets undergoing formation in the disks.

3. The ability to provide precise images at an angular resolution of 0.1 arcsec. Here the term "precise image" means being able to represent, within the noise level, the sky brightness at all points where the brightness is greater than 0.1% of the peak image brightness.

ALMA will excel at the study of chemical evolution in star-forming regions at z ~ 3, dust-gas

interactions, molecules surrounding stars, and molecular clouds. With its high sensitivity it will detect redshifted continuum dust emission out to z=10. It will reveal kinematics of obscured AGNs and quasi-stellar objects on spatial scales of 10 - 100 pc. It will use line emission from CO to measure the redshift of star-forming galaxies throughout the universe. It will image the formation of molecules and dust grains in the circumstellar shells and envelopes of evolved stars, novae, and supernovae.

ALMA's spatial resolution in the mm and sub-mm bands will be competitive with Keck's diffraction limit at wavelengths 0.6 – 2.4 μm. ALMA will be observing regions that are colder and more dense than can be seen in the visible or near-infrared with Keck. However Keck NGAO observations of H_2 and atomic hydrogen emission lines at H and K bands will complement ALMA by characterizing the warmer outer regions of molecular clouds and circumstellar disks. ALMA images and spectra of debris disks will complement the higher spatial resolution NGAO images at shorter wavelengths.

1.4 Next Generation AO Projects at Other Observatories

The NGAO team has done a survey of current and future AO systems worldwide. Within the scope of our science goals we would prefer to position Keck NGAO to take a leadership role in AO, rather than building the second or third version of a specific type of next-generation AO system.

The VLT and Gemini Observatories are planning Ground Layer AO and Extreme AO systems. Gemini South and (eventually) the LBT plan to have MCAO systems. By contrast *precision AO*, as in the planned Keck NGAO system, has not been emphasized in the plans of the other 8-10 meter telescopes.

Below in Table 1 we give an overview of plans of other observatories for what we call "next-generation AO systems" on 8 – 10 meter telescopes. By next-generation AO we mean those systems that go beyond single-conjugate AO with one laser guide star, or that aim for a special-purpose application such as high-contrast imaging or interferometry. We obtained our information from published papers, from web sites, and from the May 2006 SPIE meeting in Orlando FL.

Next-Generation AO Systems Under Development for 8 - 10 meter Telescopes					
Type	**Telescope**	**GS**	**Next-Generation AO Systems for 8 to 10 m telescopes**	**Capabilities**	**Dates**
High-contrast	Subaru	N/LGS	Coronagraphic Imager (CIAO)	Good Strehl, 188-act curvature, 4W laser	2007
High-contrast	VLT	NGS	Sphere (VLT-Planet Finder)	High Strehl; not as ambitous as GPI	2010
High-contrast	Gemini-S	NGS	Gemini Planet Imager (GPI)	Very high Strehl	2010
Wide-field	Gemini-S	5 LGS	MCAO	2' FOV	2007
Wide-field	Gemini	4 LGS	GLAO	Feasibility Study Completed	?
Wide-field	VLT	4 LGS	HAWK-I (near IR imager) + GRAAL GLAO	7.5' FOV, AO seeing reducer, 2 x EE in 0.1"	2012
Wide-field	VLT	4 LGS	MUSE (24 vis. IFUs) + GALACSI GLAO	1' FOV; 2 x EE in 0.2" at 750nm	2012
Narrow-field	VLT	4 LGS	MUSE (24 vis. IFUs) + GALACSI GLAO	10" FOV, 10% Strehl @ 650 nm	2012
Inter-ferometer	LBT	NGS	AO for LINC-NIRVANA (IR interferometer)	Phase 1: Single conj., 2 tel's Phase 2: MCAO 1 telescope Phase 3: MCAO both telescopes	Phase 1 in 2008

Table 1

Next-generation AO systems under development for 8 – 10 meter telescopes.

2 Science Cases

2.1 Multiplicity, Size, and Shape of Minor Planets

Author: Franck Marchis
Editor: Claire Max

2.1.1 Scientific background and context

While space missions largely drove early progress in planetary astronomy, we are now in an era where ground-based telescopes have greatly expanded the study of planets, planetary satellites, and the asteroid and Kuiper belts. Ground-based telescopes can efficiently perform the regular observations needed for monitoring planetary atmospheres and geology, and can quickly respond to transient events.

The study of the remnants from the formation of our solar system provides insight into the proto-planetary conditions that existed at the time of solar system formation. Such information has been locked into the orbits and properties of asteroids and Kuiper Belt objects. The study of binary (and multiple) minor planets is one key path to revealing these insights, specifically by studying their kinematics and geological properties. There are no space missions currently planned to study these binaries. This important inquiry is only accessible to ground-based telescopes with AO.

2.1.2 Scientific goals

High angular resolution studies are needed of large samples of binary asteroids to understand how their enormous present-day diversity arose from their formation conditions and subsequent physical evolution, through processes such as disruption and re-accretion, fragmentation, ejecta capture, and fission. Specifically one can study:

- Formation and interiors of minor planets by accurate estimates of the size and shape of minor planets and their companions
- Mass, density, and distribution of interior material by precise determination of the orbital parameters of moonlet satellites
- Chemical composition and age, by combining high angular resolution with spectroscopic analysis

2.1.3 Proposed observations and targets

2.1.3.1 Size and shape

Spatially resolved imaging of large asteroids is critical in order to derive reliable statistical constraints on large collisions throughout the Main Belt. Observations of the 15 or 20 largest asteroids would provide the statistics necessary to put much stronger constraints on the frequency of major collisions. We estimate that 20 Main Belt asteroids will be resolved with sufficient resolution with NGAO in R-band (33 in V-band) to obtain mapping comparable to

that already done for 4 Vesta.

Table 2 summarizes the number of asteroids resolvable from visible to near-IR, categorized by domain and population. Thanks to NGAO's high angular resolution in V and R bands, ~800 main-belt asteroids could be resolved and have their shape estimated with a precision of better than 7%. With the current AO system ~100 asteroids, located only in the main-belt, can be resolved. The determination of the size and shape of even a few Trojan asteroids will be useful to estimate their albedo. For Near Earth Objects (NEAs), the large number of resolvable objects is a result of very close approaches to Earth.

Table 2
Number of asteroids resolvable with Keck NGAO in various wavelength ranges and populations (assuming on-axis observations).

Populations by brightness (numbered and unnumbered asteroids)					
Orbital type	Total number	V < 15	15 < V < 16	16 < V < 17	17 < V < 18
Near Earth	3923	1666	583	622	521
Main Belt	318474	4149	9859	30246	88049
Trojan	1997	13	44	108	273
Centaur	80	1	1	2	2
TNO	1010	1	2	0	2
Other	3244	140	289	638	870

This research program will have even higher impact if it is combined with the study of binary asteroids. Recent studies suggest that the primary asteroid of most binary asteroid systems has a rubble-pile structure, indicating that they have weak shear strength (Marchis et al., 2006). Consequently their shape is directly related to the angular momentum at their formation (Tanga et al., 2006). One can obtain their mass through determination of moonlet orbits combined with a good shape determination, by direct imaging in the visible (which provides the best angular resolution). Assuming an R band Strehl > 20% so that there is a clear diffraction-limited peak in the PSF, we estimate that between 1000-4000 new binary asteroids could be discovered with NGAO. An accurate shape estimate for ~300 of them (an order of magnitude more than the number of asteroids with currently known shapes) can be attained with NGAO in R band. Six observations taken at various longitudes are enough to accurately reconstruct the 3D-shape of the asteroid. Twelve nights of observations should be considered for the completion of such a program. Dedicated nights are not necessary since this program can be combined with the study of satellite orbits of asteroids using the same instrumentation.

2.1.3.2 Orbits of multiple asteroidal systems

Study of main-belt multiple systems: One of the main limitations of current AO observations for a large search for binary asteroids and for characterization of their orbits is the limited quantity number of asteroids observable considering the magnitude limit on the NGS wavefront sensor. The Keck NGS AO system can use guide stars down to 13.5 magnitude, so ~1000 main-belt asteroids (to perihelion >2.15 AU and aphelion <3.3 AU) can be observed.

With NGAO providing an excellent correction up to tip-tilt star magnitudes V = 17 or J = 19 10% of the known main-belt population can be searched, corresponding to the potential

discovery of 1000 multiple systems assuming the current multiplicity rate of 6% - 15%. This is a lower limit on the detection rate of new moonlets, because the NGAO system will provide a more stable correction than current Keck LGS AO and the halo due to uncorrected phase errors will be significantly reduced.

Closer and fainter satellites should be detectable, as will be explained below. At the time of this writing, the orbits of ~15 visual binary systems are known and display considerable diversity. To better understand these differences, we propose to focus our study on 100 new binary systems in the main-belt discovered elsewhere, by light-curves or snap shot programs on HST and/or previous AO systems. The increase by an order of magnitude of known orbits will help us to understand how they formed as members of a collisional family, their distance to the Sun, their size and shape, and other parameters.

To reach a peak SNR~1000-3000 on an AO image, the typical total integration times assuming 140 nm of wavefront error are 5 min and 15 min for 13th or 17th V-magnitude targets respectively. Considering a current overhead of 25 min (Marchis et al. 2004b) to move the telescope onto the target and close the AO loop, the total telescope time per observation is ~30 min. This overhead time should be significantly improved by careful design of the NGAO system. The orbit of an asteroid can be approximated (P, a, e, i) after 8 consecutive observations taken over a period of 1-2 months to limit the parallax effect, corresponding to the need for 0.3 nights per object. Thirty nights of observation would be requested for this program over 3 years.

To illustrate the gain in quality expected with NGAO, we generated a set of simulated images of the triple asteroid system 87 Sylvia. The binary nature of this asteroid was discovered in 2001 using the Keck NGS AO system. Marchis et al. (2005) announced recently the discovery of a smaller and closer moonlet. The system is composed of a D=280 km ellipsoidal primary around which two moons describe a circular and coplanar orbit: “Romulus”, the outermost moonlet (D=18 km) at 1356 km (~0.7”) and “Remus” (D = 7 km) at 706 km (~0.35”). In our simulation we added artificially two additional moonlets around the primary: “S1/New” (D=3.5 km) located between Romulus and Remus (at 1050 km) and “S2/New” (D=12 km) closer to the primary (at 480 km). This system is particularly difficult to observe since the orbits of the moons are nearly edge-on. We blurred the image using the simulated NGAO and Keck NGS AO PSFs (with an rms error of 140 nm) and added Poisson and detector noise to reach a S/N of 2000 (corresponding to 1-3 min integration time for a V=12 target). We then estimated whether the moonlets could be detected and their intensity measured by aperture photometry. Figure 1 displays a comparison for one observation between the current Keck NGS AO, NGAO in two wavelengths, and HST/ACS. The angular resolution and thus the sensitivity of the NGAO R-band is a clear improvement and permits detection of the faintest moon of the system.

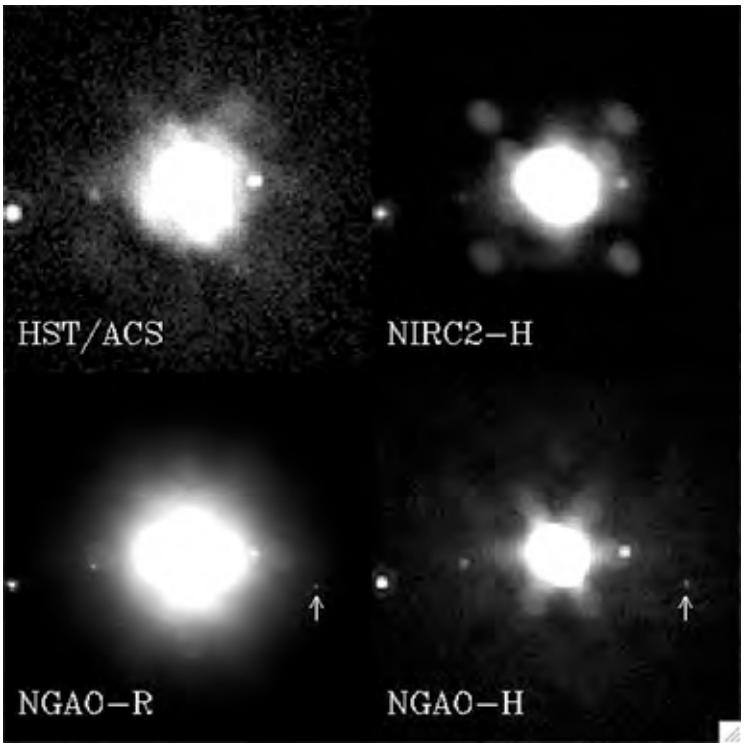

Figure 1
Simulation of pseudo-Sylvia observed with various AO systems.
We assumed that NGAO has a wavefront error of 140 nm in this simulation.

Table 3 summarizes the 2-σ detection rate for the pseudo-Sylvia system moonlets. The photometry was done using the same technique as for real observations (aperture photometry + fitting/correction of flux lost). The detection rates for NGAO- R band are 100% for all moons. One can also notice a very good photometric recovery with this AO system. The chances to discover multiple systems and to analyze them are significantly improved with NGAO. It should be also emphasized that because the astrometric accuracy is also better, determination of the orbital elements of the moons will be also more accurate (e.g., a significant eccentricity or small tilt of the orbit).

Table 3
Detection rate and photometry on the moons of pseudo-Sylvia, assuming an NGAO system with 140 nm of wavefront error.

	Romulus		Remus		S_New1		S_New2	
	Det. rate	Δm	Det. Rate	Δm	Det. Rate	Δm	Det. Rate	Δm
Perfect image	100%	6.6	100%	8.1	100%	6.9	100%	9.6
NIRC2-H	82%	6.4±0.04	70%	8.3±0.3	11%	6.9±0.2	0%	N/A
NGAO-H	100%	7.0±0.1	70%	8.5±0.5	40%	7.1±0.2	0%	N/A
NGAO-R	100%	6.60±0.01	100%	8.3±0.1	100%	6.9±1.1	100%	10.1±0.3

2.1.4 AO requirements

2.1.4.1 Wavefront error

A wavefront error of 140 nm would provide excellent angular resolution in the visible, better than HST and adequate for our program. We expect excellent sensitivity for point source detection. Table 14 of the Keck NGAO Proposal to the SSC (June 2006) indicates that the point source limiting magnitude for such AO system (5σ, 1hr integration) is 29.0 in R band. For comparison, recent observations of Pluto-Charon recorded with ACS/WFC at 0.61 μm (Weaver et al. 2006) allowed the detection of 2 new moons with R = 23.4 (SNR=35). With NGAO in R band with 140 nm of wavefront error, these moons could have been discovered with SNR~47. Such gain in sensitivity will help find more multiple systems, and also to find out if around these multiple systems there is still a ring of dust left over from the catastrophic collision that formed the multiple system. We are currently carrying out simulations to characterize the science that could be done with 170 nm and 200 nm of wavefront error. Our expectation is that there will not be a "cliff" in science output as the wavefront error degrades, but rather a gradual decrease in the number of moonlets detected and in the number of primary asteroids whose shapes can be measured. Future releases of this Science Case Requirements Document will compare the science performance for 140, 170, and 200 nm of wavefront error.

2.1.4.2 Encircled energy

N/A

2.1.4.3 Contiguous field requirement

Required FOV is ≤ 2 arc sec. There is no requirement for a larger contiguous field.

2.1.4.4 Photometric precision

Accurate photometry will lead to a better estimate of the size and shape of the moonlets, which will give strong constraints on their formation mechanism (e.g. one would be able to tell if the moonlet is synchronized and displays an equilibrium shape under tidal forces). The proposed method is to detect photometric changes due to its potential lack of sphericity over the moonlet's orbit, as we see different faces of the moonlet. With current AO systems, the photometric accuracy on the moonlet is rather poor. The accuracy of the flux estimate of the 22 Kalliope moonlet, orbiting at 0.6 arc sec with $\Delta m=3$, was only ~20% with Keck LGS AO. Assuming the same sky background and detector noise as with current Keck LGS AO, NGAO in the near IR is predicted to yield a photometric accuracy of 5% or better for the same observing situation.

2.1.4.5 Astrometric precision

The astrometric measurements for our program are relative to the primary. The maximum angular separation between the secondary and the primary is 0.7 arc sec. We require the visible instrument to provide images with at least Nyquist sampling. The relative position of the secondary, estimated by a Moffat-Gauss fit, cannot be better than a 1/4 of a pixel (since the primary is resolved). The residual distortion over the field of the detector should not be more than 1.5 mas. Uncharacterized detector distortion will be the limiting factor in these astrometric measurements.

2.1.4.6 Contrast

At the current time the faintest and closest moonlet discovered around an asteroid is Remus, orbiting at 0.2-0.5" (350-700 km) around 87 Sylvia with Δm (peak-to-peak) = 3.5. The detection of this moonlet is challenging with current Keck AO, and also with the VLT NACO system. For instance, it was detected (SNR > 3) on 10 images out of 34 recorded over 2 months with the VLT. A better contrast will increase the detection rate, allowing us to see fainter and closer moonlets but also to get a better photometric measurement on those already known. Coronagraphic observations cannot be considered in our case: the central source is not point-like so the effect of the mask will be negligible. It is assumed that the distance to the primary of a satellite is driven by tidal effects, but at the moment theoretical work fails to agree on the age of an asteroid and the position of its moonlet. This is mostly due to the lack of observed systems in which a moonlet orbits at less than 1000 km ($a / R_p < 8$). Two orders of magnitude gain in the detection limit ($\Delta m = 5.5$ at 0.5 arc sec) would lead to the possibility of detecting a half-size moonlet around (87) Sylvia. **Polarimetric precision**

N/A

2.1.4.8 Backgrounds

Any background equal to or better than current Keck AO will be acceptable. Lower

backgrounds are always better.

2.1.4.9 Overall transmission

Comparable to or better than with current LGS AO system.

2.1.5 Other key design features

2.1.5.1 Required observing modes

The capability of efficiently observing moving targets must be included in the design of NGAO, so that implementation of differential guiding when the tip-tilt source is not the object itself (and is moving relative to the target) is possible. The maximum relative velocity to be expected is 70 arc sec per hour.

We also point out that for this science case, the scientific return of the Keck telescope and the NGAO system would greatly improve if some sort of flexible or queue scheduling or service observing were to be offered. With an error budget of 140 nm the NGAO system will achieve a Strehl of ~20% in R- band under moderate seeing conditions. Bright targets like the Galilean satellites (V~6) can be observed even if the seeing conditions are lower than average in the near IR (at separations > 1.2"). Other difficult observations, such as the study of multiple TNOs (V>17) could be scheduled when the seeing conditions were excellent (< 0.7"). Finally, frequent and extremely short (half hour) direct imaging observations of a specific target such as Io, to monitor its activity over a long period of time, would be extremely valuable and are not available on HST. All these programs could be done more easily if flexible or queue or service observing were available at Keck. It would also relax the constraints on the NGAO error budget since it would be possible to take advantage of excellent atmospheric conditions to observe the faintest objects.

2.1.5.2 Observing efficiency

Current observations with Keck AO have a ~25 minute overhead when switching between targets for an on-axis LGS observation of an asteroid. It is very desirable to reduce this overhead. A goal of 10 minutes setup time when switching between LGS targets is desirable. There is no firm requirement, but observing efficiency suffers in direct proportion to the time it takes to switch from one target to the next, particularly when the observing time per target is relatively short. This is an important constraint for this science case, since numerous targets must be observed per night.

2.1.6 Instrument requirements

2.1.6.1 Required instruments

Primary: Visible imager, on-axis, diffraction limited, narrow field, with coronagraph
Secondary: Near IR imager, on-axis, diffraction limited, narrow field, with coronagraph
Secondary: IFU, on-axis, narrow field, R~100 for visible wavelengths
Secondary: IFU, on-axis, narrow field, R~1000-4000 for near infrared wavelengths

2.1.6.2 Field of view

No more than 2 arc sec.

2.1.6.3 Field of regard

Should be determined by the requirement to find adequate tip-tilt stars.

2.1.6.4 IFU multiplicity

Single object mode only. Density of asteroids on the sky is not high enough for multi-object observing.

2.1.6.5 Wavelength coverage

Imaging: Wavelengths 0.7 – 2.4 μm
Spectroscopy: Wavelengths 0.8 – 2.4 μm

2.1.6.6 Spectral resolution

There are spectroscopic features at visible wavelengths (e.g. the absorption bands of pyroxene at 0.85 - 1 μm). For these bands, which are relatively broad, a spectral resolution of R~100 is desirable. There are also bands in the near IR. SO_2 frost (bands at 1.98 and 2.12 μm) can be best observed with R~1000. However R~4000 would be acceptable.

2.1.7 References

Marchis, F., J. Berthier, P. Descamps, et al. 2004b. Studying binary asteroids with NGS and LGS AO systems, SPIE Proceeding, Glasgow, Scotland, 5490, 338.

Marchis, F., Descamps, P., Hestroffer, D. et al., 2005. Discovery of the triple asteroidal system 87 Sylvia, *Nature* 436, 7052, 822.

Marchis, F.; Kaasalainen, M.; Hom, E. F. Y.; Berthier, J.; Enriquez, J.; Hestroffer, D.; Le Mignant, D.; de Pater, I. 2006. Shape, size and multiplicity of main-belt asteroids, *Icarus* 185, 39.

Tanga, Paolo; Consigli, J.; Hestroffer, D.; Comito, C.; Cellino, A.; Richardson, D. C. 2006, Are Asteroid Shapes Compatible With Gravitational Reaccumulation? American Astronomical Society, DPS meeting #38, #65.06

Weaver, H. A.; Stern, S. A.; Mutchler, M. J.; Steffl, A. J.; Buie, M. W.; Merline, W. J.; Spencer, J. R.; Young, E. F.; Young, L. A. 2006, Discovery of two new satellites of Pluto, Nature, 439, 943.

2.2 Imaging and characterization of extrasolar planets around nearby stars

Author: Michael Liu
Editor: Claire Max

2.2.1 Scientific background and context

The unique combination of high-contrast near-IR imaging (K-band Strehl ratios of 80-90%) and large sky coverage delivered by NGAO will enable direct imaging searches for Jovian-mass planets around nearby young low-mass stars and brown dwarfs. Both the Gemini Observatory and ESO are developing highly specialized planet-finding AO systems with extremely high contrast for direct imaging of young planets. These "extreme AO" systems are very powerful, but their design inevitably restricts them to searches around bright, solar-type stars (I=8 to 9 mag).

NGAO will strongly distinguish work at WMKO from all other direct imaging searches planned for large ground-based telescopes. By number, low-mass stars ($M \leq 0.5\ M_{Sun}$) and brown dwarfs dominate any volume-limited sample, and thus these objects may represent the most common hosts of planetary systems. Such cool, optically faint targets will be unobservable with specialized extreme AO systems because their parent stars are not bright enough to provide a high-order wavefront reference. But thousands of cool stars in the solar neighborhood can be targeted by NGAO. Direct imaging of extrasolar planets is substantially easier around these lower mass primaries, since the required contrast ratios are smaller for a given companion mass.

2.2.2 Scientific goals

Direct imaging of extrasolar planets by NGAO would allow us to measure their colors, temperatures, and luminosities, thereby testing theoretical models of planetary evolution and atmospheres. NGAO spectroscopic follow-up will be an important means to characterize the atmospheres of extrasolar planets, which are otherwise essentially inaccessible to spectroscopy. Figure 2 summarizes the relative parameter space explored by NGAO and extreme AO. The complementarity of the two systems is very important: establishing the mass and separation distribution of planets around a wide range of stellar host masses and ages is a key avenue to understanding the planet formation process. The optical faintness of low-mass stars, brown dwarfs and the very youngest stars make them inaccessible to extreme AO systems but excellent targets for NGAO.

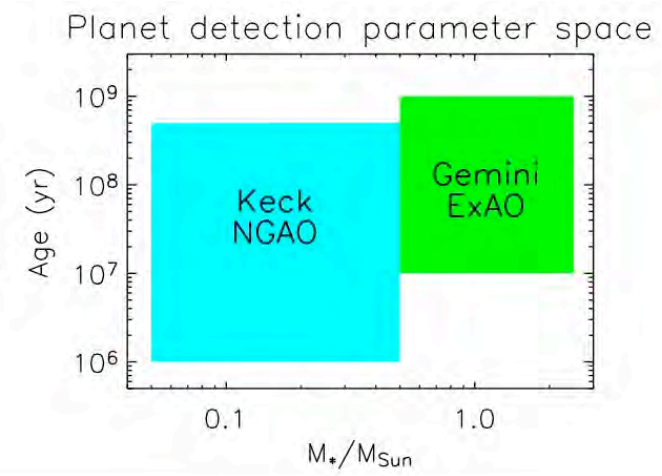

Figure 2 Schematic illustration of the parameter space of Keck NGAO and of the Gemini Planet Imager for direct imaging of extrasolar planets.

2.2.2.1 Planets around low-mass stars and brown dwarfs

Direct imaging of substellar companions (brown dwarfs and extrasolar planets) is substantially easier around lower mass primaries, since the required contrast ratios are smaller for a given companion mass. Indeed, the first bona fide L dwarf and T dwarfs were discovered as companions to low-mass stars (Becklin & Zuckerman 1988, Nakajima et al. 1995). Thus, searching for low-mass stars and brown dwarfs is an appealing avenue for planet detection and characterization. Given that low-mass stars are so much more abundant than higher mass stars, they might constitute the most common hosts of planetary systems. Figure 3 shows an estimate of the planet detection sensitivity for NGAO.

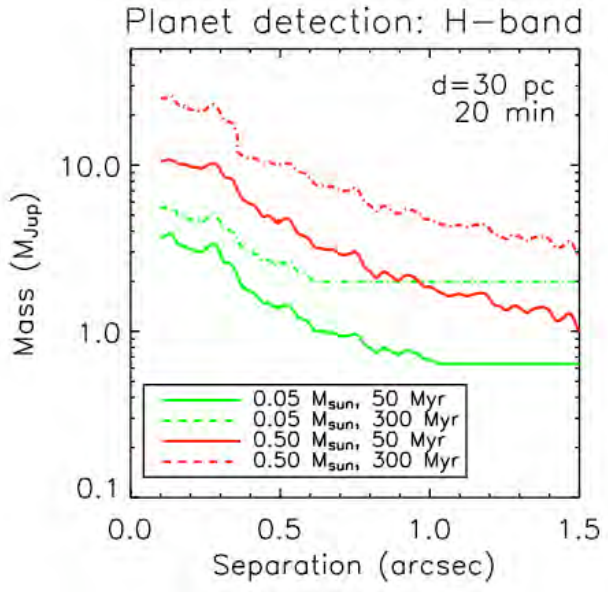

Figure 3

Estimated NGAO sensitivity for direct imaging of planets around low-mass stars (red lines) and brown dwarfs (green lines). NGAO will be able to search for Jovian-mass companions around large numbers of low-mass stars and brown dwarfs in the solar neighborhood

Spectroscopic follow-up of the coldest companions will be an important path in characterizing the atmospheres of objects in the planetary domain. Strong molecular absorption features from water and methane provide diagnostics of temperature and surface gravity at modest (R~100) spectral resolution. Below ~500 K, water clouds are expected to form and may mark the onset of a new spectral class, a.k.a. "Y dwarfs". Such objects represent the missing link between the known T dwarfs and Jupiter, but are probably too faint and rare to be detected as free-floating objects in shallow all-sky surveys such as 2MASS and SDSS. Furthermore, the coolest/lowest mass objects may not exist as free-floating objects if there is a low-mass cutoff to the initial mass function of the star formation process, e.g., from opacity-limited fragmentation of molecular clouds (M_{min} ~ 5-10 M_{Jup}; Silk 1977). Even cooler/lower mass objects might only form via fragmentation, akin to the formation of binary stars, and may only be found as companions.

2.2.2.2 Very young planets in the nearest star-forming regions

Imaging searches and characterization at the very youngest (T Tauri) stages of stellar evolution provide a unique probe of the origin of extrasolar planets, by constraining their formation timescales and orbital separations. Young stars and brown dwarfs can be enshrouded by substantial dust extinction, both from the natal molecular cloud and their own circumstellar material. Thus most young (T Tauri) stars are too optically faint for current NGS AO systems or future ExAO systems. Keck NGAO imaging will probe physical separations of ≥ 5-10 AU around these stars.

It is still an open question whether giant planets form extremely rapidly (≤ 10^4 yr) due to disk instabilities (e.g. Boss 1998) or if they first assemble as ~10 M_{earth} rocky cores and then accrete ~300 M_{earth} of gaseous material over a total timescale of ~1-10 Myr (e.g. Lissauer 1998). Potentially both mechanisms may be relevant, depending on the range of orbital separations and circumstellar disk masses. In addition, imaging searches of both young T Tauri stars with disks (classical TTS) and without disks (weak TTS) can help to constrain the formation timescale. In particular, weak T Tauri stars with planetary companions would suggest that planet formation could occur even when disk evolution/dissipation happens rapidly.

2.2.3 Proposed observations

See above description.

2.2.4 AO and instrument requirements

The **high contrast near-IR (0.9-2.5 micron) imaging** required for planet imaging will require coronagraphy to suppress PSF diffraction features.

In many cases**, near-IR tiptilt sensing** is required given the intrinsic redness of the science targets (e.g. brown dwarfs) or the high extinction of the science regions (e.g. star-forming regions). **Both on-axis and off-axis tip-tilt sensing will be needed**, depending on the optical/IR brightness of the primary stars. For off-axis science applications, sky coverage of >30% (as an areal average over the entire sky) is needed at the highest image quality over a corrected field of view < 5" in size.

Low-resolution (R~100) near-IR (0.9-2.4 micron) spectroscopy is essential to follow-up planet discoveries, in order to determine their temperatures, surface gravities, and masses. The relevant spectral features have broad wavelength ranges, e.g. the broad-band SEDs of circumstellar dust needed to diagnose grain composition and sizes and the broad molecular absorption band of H_2O and CH_4 present in the atmospheres of ultracool brown dwarfs and extrasolar planets. **Thermal (L-band) imaging** would be desirable to help measure the SEDs of the planets, but is not essential for this science.

2.2.5 Performance Requirements

2.2.5.1 Wavefront error

The key performance driver for this science case is contrast, not wavefront error. Initial simulations with an RMS wavefront error of 140 nm indicated that the required contrast could be achieved. Simulations are under way to understand how the science would degrade for wavefront errors of 170 and 200 nm (relative to 140 nm). Good control and calibration of internal static wavefront calibration errors will also be required of the AO system.

2.2.5.2 Encircled energy

N/A

2.2.5.3 Need for large contiguous fields

Required FOV is only a few (< 5) arc sec. A larger contiguous field is not required.

2.2.5.4 Photometric precision

Probably not a key requirement. Require relative photometry of planetary companion to primary star of better than 0.05 mag, or absolute photometry of planetary companion to the same accuracy.

2.2.5.5 Astrometric precision

Probably not a key requirement. Astrometric accuracy to ~1/10 of the PSF FWHM would suffice for proper motion confirmation that candidate planets are physically associated to their primaries.

2.2.5.6 Contrast

From a science standpoint, the required contrast can be set by the need to directly image Jupiter-mass planets around a large sample of (1) field low-mass stars and brown dwarfs at ages of <~200 Myr and (2) young stars in the nearest star-forming regions. A benchmark value of $\Delta H=13$ magnitudes at 1 arc sec separation is required.

2.2.5.7 Polarimetric precision

N/A

2.2.5.8 Backgrounds

Thermal L-band photometry is desirable, but not a key requirement. Backgrounds lower than those on the current Keck AO system would be helpful for L-band photometry.

2.2.5.9 Overall transmission

For some targets with low-mass primaries (brown dwarfs) and relatively old ages, high sensitivity will be a benefit at separations of ≥ 1 arc sec. The baseline sensitivity numbers from the NGAO proposal of H=25 mag (5-sigma) in 20 minutes of on-source integration time are suitable for these purposes.

2.2.6 Other key design features

2.2.6.1 Required observing modes

Imaging with both on-axis and off-axis tip-tilt stars, and single-object spectroscopy will be needed. Coronagraphic imaging is required, and will need additional design consideration because one must be able to center the science target on the focal plane mask and to keep it there during the observations.

2.2.6.2 Observing efficiency

Good efficiency is required, i.e. 10 min or less overhead per target, since we want to be able to observe many (several dozen) targets per night.

2.2.7 Instrument requirements

2.2.7.1 Instruments needed

Primary: Near-IR diffraction limited imager, narrow field, 0.9-2.4 microns, coronagraph
Secondary: Near-IR IFU, R~100, diffraction limited, 0.9-2.4 microns, coronagraph?
Secondary: L-band imager

2.2.7.2 Field of view

No more than 5 arc sec for both the near IR imager and the R~100 IFU.

2.2.7.3 Field of regard

Determined by the need for tip-tilt stars. All-sky average sky coverage for off-axis observations should be >30%.

2.2.7.4 IFU multiplicity

One object at a time only.

2.2.7.5 Wavelength coverage

0.9-2.4 microns (extension to L-band desirable, but not essential).

2.2.7.6 Spectral resolution

R~100 at 0.9-2.4 microns.

2.2.8 References

Becklin, E. & Zuckerman, B. 1988, Nature 336, 656

Boss, A. 1998, ApJ 503, 923

Lissauer, J. 1998, in "Origins," ASP Conf. Series vol. 148, 327

Nakajima, T. et al. 1995, Nature 378, 463

Silk, J. 1977, ApJ 214, 152

2.3 Precision Astrometry: Measurements of General Relativity Effects in the Galactic Center

Authors: Andrea Ghez and Jessica Lu
Editor: Claire Max

2.3.1 Scientific background and goals

The proximity of our Galaxy's center presents a unique opportunity to study a massive black hole (BH) and its environs at much higher spatial resolution than can be brought to bear on any other galaxy. In the last decade, near-IR observations with astrometric precisions of < 1 mas and radial velocity precision of 20 km/s have enabled the measurement of orbital motions for several stars near the Galactic center (GC), revealing a central dark mass of 3.7×10^6 M_{Sun} (Ghez et al. 2003, Ghez et al. 2005; Schodel et al. 2002; Schodel et al. 2003). Radio VLBA observations have now resolved the central object to within several multiples of the event horizon, indicating that the central mass is confined to a radius smaller than 1 AU (Shen et al. 2005). These observations provide the most definitive evidence for the existence of massive BHs in the centers of galaxies. The orbital motions now also provide the most accurate measurement of the GC distance R_0, constraining it to within a few percent (Eisenhauer et al. 2003).

2.3.2 General Relativistic Effects

Due to the crowded stellar environment at the GC and the strong line-of-sight optical absorption, tracking the stellar orbits requires the high angular resolution, near-IR imaging capabilities of adaptive optics on telescopes with large primary mirrors, such as Keck. Though the current orbital reconstructions are consistent with pure Keplerian motion, with improved astrometric and radial velocity precision deviations from pure Keplerian motion are expected. With Keck NGAO we will be able to detect the deviations from Keplerian motion due to a variety of effects. These will provide a unique laboratory for probing the dynamics of galactic nuclei, the properties of exotic dark matter, and the mass function of stellar-mass black holes. They will also provide the first tests of general relativity in the high mass, strong gravity, regime. Keck NGAO will measure these non-Keplerian motions to precisions that will not be greatly surpassed even in the era of extremely large (~30m) telescopes.

Of the theories describing the four fundamental forces of nature, the theory that describes gravity, general relativity (GR), is the least tested. In particular, GR has not been tested in the strong field limit, on the mass scale of massive BHs. The highly eccentric 15 yr orbit of the star S0-2 brings it within 100 AU of the central BH, corresponding to ~1000 times the BH's Schwarzschild radius (i.e., its event horizon). Studying the pericenter passage of S0-2 and the other high eccentricity stars therefore offers an opportunity to test GR in the strong gravity regime.

With Keck NGAO, the orbits can be monitored with sufficient precision to enable a measurement of post-Newtonian general relativistic effects associated with the BH. This includes the prograde precession of orbits. As Figure 1 illustrates, the General Relativistic prograde precession can be measured even for single orbits of known stars (e.g., S0-2, K=14.1 mag) if we have an astrometric precision of ~ 100 μas coupled with a radial velocity precision of 10 km/s.

With Keck NGAO, the orbits can be monitored with sufficient precision to enable a measurement of post-Newtonian general relativistic effects associated with the BH. This includes the prograde precession of orbits. As Figure 4 illustrates, the General Relativistic prograde precession can be measured even for single orbits of known stars (e.g., S0-2, K=14.1 mag) if we have an astrometric precision of ~ 100 μas coupled with a radial velocity precision of 10 km/s.

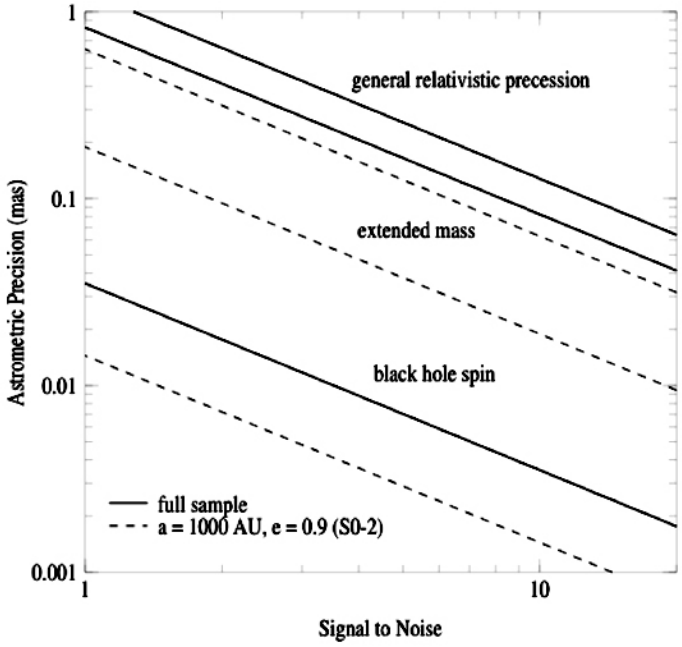

Figure 4

Required astrometric precision for detecting, from top to bottom, GR effects associated with relativistic prograde precession, extended mass within the stellar orbits, and frame-dragging effects due to BH spin (based on Weinberg et al. 2005). Estimates are based on measurements of stellar orbits and positions from Keck diffraction-limited images (thick, solid lines), and assume radial velocity measurement errors of 10 km/s. The stellar orbits include 16 stars within 0.5" of Sgr A* with orbital fits obtained from speckle imaging measurements and 142 stars within 1" of Sgr A* with stellar positions obtained with new, deep AO maps. For comparison, we also show estimates based on measurements from just the short-period star S0-2 (thin, dashed line). Results are for a 10-year baseline with 10 integrations per year. Low-order GR and extended matter effects are detectable at the >7σ level if an astrometric precision of ~100 μas can be achieved. Detection of BH spin requires either better precision or, at ~100 μas precision, improved SNR obtained by observation of multiple as-yet-undiscovered high-eccentricity, short-period stars over multiple orbits.

Keck NGAO will bring several important improvements to measurements at the Galactic Center:

1) Current measurements are strongly confusion limited, because the Galactic Center is a very crowded field. Higher Strehl at K-band will improve contrast and therefore reduce the confusion, improving both photometric and astrometric accuracy because the previously undetected faint star population will cause less of a bias in the positions and magnitudes of brighter stars.

2) Higher Strehl at K-band will allow the detection of new stars, some of which may pass close enough to the black hole to contribute to the obtainable accuracy and precision of General Relativistic effects. (See figure caption.)

3) NGAO's use of multiple laser guide stars and multiple IR tip-tilt stars will decrease the field dependence of the PSF, thereby increasing both photometric and astrometric accuracy. This effect needs be quantified.

4) The accuracy of current radial-velocity measurements is limited by signal to noise. NGAO's higher Strehl and lower sky background will materially improve the radial-velocity contribution to orbit determinations.

2.3.3 R_0 and the dark matter halo

Since the orbital periods are proportional to $R_0^{3/2}M_{bh}^{-1/2}$ and the radial velocities are proportional to $R_0^{-1/2}M_{bh}^{1/2}$, where R_0 is the heliocentric distance to the BH and M_{bh} its mass, the two parameters are not degenerate and can be determined independently (Salim & Gould 1999). As shown in Figure 4, by complimenting high precision astrometric measurements with high precision radial velocity measurements with accuracies of ~10 km s^{-1}, we can measure R_0 to an accuracy of only a few parsecs (i.e., ~0.1% accuracy) with Keck NGAO. Today's radial velocity precision for the observations in hand is about 20 km/s. This could be improved to 10 km/sec with higher signal to noise observations, either from longer integration times or lower backgrounds.

Since R_0 sets the scale within which is contained the observed mass of the Galaxy, measuring it to high precision enables one to determine to equally high precision the size and shape of the Milky Way's several kpc-scale dark matter halo (Olling & Merrifield 2000). The halo shape tells us about the nature of dark matter (e.g., the extent to which it self-interacts) and the process of galaxy formation (how the dark matter halo relaxes following mergers). Currently the shape is very poorly constrained.

2.3.4 Proposed observations and targets

Target: Central 10 arc sec of the Galactic Center, centered on SgrA*. Note that this is a low-elevation target from Keck (RA 17 45 40 DEC -29 00 28).

Observing wavelengths: K band (2.2 microns)

Observing mode: Imaging for astrometry purposes, and spectroscopy for radial velocities

2.3.5 Observing plan for Astrometric Imaging:

Based upon the way things are done today using 1st-generation Keck AO:

a) Guide Star Aquisition:

Current visible-wavelength guide star is USNO-A2.0 0600-28577051 (R=14.0, Separation = 19.3'')

There are a great many possible IR tip-tilt stars, as shown in Appendix A. The addition of multiple IR-corrected tip-tilt stars is anticipated to improve astrometric accuracy considerably, although more work is needed in order to understand the specific limitations of today's observations.

b) 1-minute K' exposures, continuing for 3.5 hours elapsed time

c) Dither pattern is random over a 0.7'' box (small box used to minimize distortion)

d) Construct 40 arcsec mosaics to tie to radio astrometric reference frame (radio masers)

e) After the Galactic Center has set, move to a dark patch of sky at a similar airmass to obtain sky exposures.

Standard stars: none (astrometry)

Data Analysis:

1. Image reduction is standard, including distortion correction using the NIRC2 pre-ship review distortion solution. Improved distortion solution is needed and appears to be possible with data in hand.
2. Individual exposures are shifted (translations only) and added together for an entire night to produce a final map. Information from >1000 stars is included in the solution.
3. Individual exposures are also divided into 3 subsets of equal quality to produce 3 images used for determining the astrometric and photometric RMS errors.
4. Source extraction is performed using StarFinder (Diolaiti et al 2000) which iteratively estimates the PSF from several bright stars in the image and then extracts all source positions and photometry.
5. Star lists from different epochs are aligned by matching all the stars and minimizing the quad-sum of their offsets allowing for a 2nd order transformation between epochs.

2.3.6 Observing plan for Radial Velocity Measurements (IFU spectroscopy):

K-band IFU spectroscopy, one field
20 or 35 mas plate scale, R~4000

FOV at least 1.0'' x 1.0''
Exposure times are currently 15 minutes.
Sky frames of the same duration are obtained in the same mode after the Galactic Center sets in order to remove OH lines.
Obtain standards stars of A and G spectral type to remove telluric lines.
Data analysis performed with a provided pipeline to do wavelength calibration.

2.3.7 Current issues and limitations that could be further explored with existing data sets

1) Improved geometric distortion map for narrow camera on NIRC2. At present we know that the map from pre-ship review is incorrect at the half-pixel level.

2) Effect of differential tip-tilt error across 10 arc sec field. Present data show the expected decrease in astrometric errors as the stars get brighter (K=20 -> 15), due to photon noise improvement. However for stars brighter than K=15, the astrometric error hits a plateau and does not improve further as the stars get brighter. This is illustrated in Figure 5. The Galactic Center Group at UCLA has three hypotheses for the existence of this floor: differential tip-tilt anisoplanatism across the field, differential high-order anisoplanatism across the field, and/or lack of a good enough distortion solution for the narrow camera. At present the Galactic Center Group thinks the most likely cause is differential tip-tilt anisoplanatism; they plan to test this hypothesis by further analysis of existing data.

3) In principle chromatic and/or achromatic atmospheric refraction could be adversely affecting current accuracy. These effects will also be analyzed further.

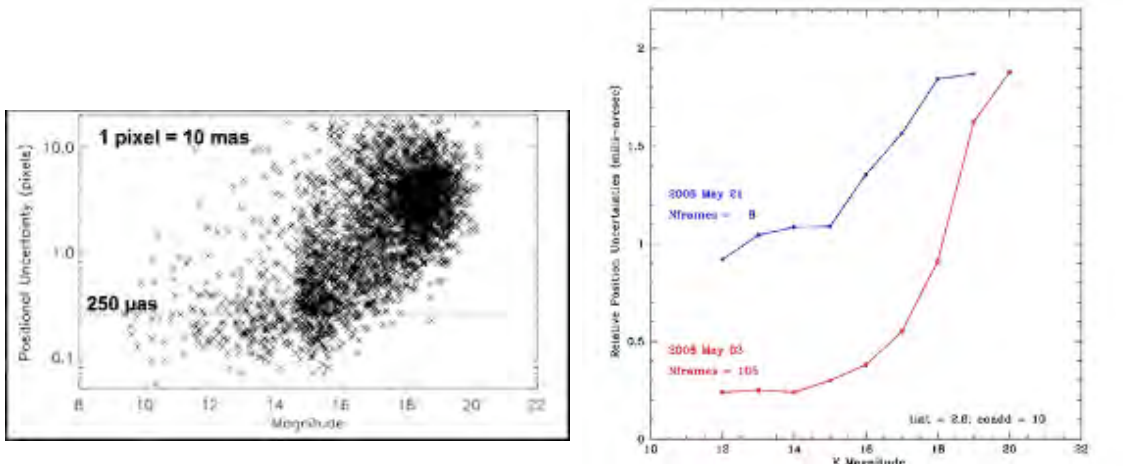

Figure 5
Left panel: positional uncertainty vs. stellar magnitude for stars near Galactic Center. Pixel scale is 0.01 arc sec/px. Right panel: average values of positional uncertainties for two different data sets. The positional uncertainty of the "floor" changes from about 1 mas to 0.25 mas between the two data sets shown.

2.3.8 AO requirements

Astrometry:

Astrometric precision	100 micro arc sec or better Wavefront error 170 nm or better
Tip-tilt correction	IR tip-tilt needed; due to very strong reddening in Galactic Center, available J-band stars will be fainter than at H or K band, so either H or K is desirable for tip-tilt sensors. The total astrometric precision should be better than 0.1 mas. Therefore the required contribution from differential tip-tilt must be smaller than this. Further investigation into the astrometric error budget is required to determine the exact requirement.
Photometric precision	na
Polarimetric precision	na
Backgrounds	na (confusion dominated)

2.3.9 General comments on astrometric accuracy in an AO system with multiple deformable mirrors

One of the point design concepts for Keck NGAO specifies a large-stroke deformable mirror within the main optical relay, plus a high-order MEMS deformable mirror either located on-axis or in multiple deployable IFU arms. Any AO system with multiple DMs must consider the impacts on astrometric accuracy. The following is a quote from the TMT Science-Driven Requirements Document that seems relevant to Keck NGAO design as well (this should be regarded as a place-holder for future NGAO-specific analysis of the same topic):

"An astrometric MCAO system must constrain Zernike modes 4-6 using either a single natural guide star (NGS) which is bright enough to sense defocus and astigmatism or provide two additional tip-tilt stars, making their total number 3. The differential tilts between the three tip-tilt stars constrain these modes. This requirement occurs because the tip and tilt of laser guide stars (LGS) are undetermined. As a consequence, the information brought by them is insufficient for a full solution of the tomographic problem. In addition to tip and tilt, differential astigmatism and defocus between the two DMs is unconstrained. These three unconstrained modes do not influence on-axis image quality, but produce differential tilt between the different parts of the field of view.

If multiple tip-tilt sensors are used, the MCAO system must provide for a facility to align them. If the tip-tilt sensors for the three NGSs are misplaced, the MCAO system will compensate these errors in the closed loop, hence the field will be distorted. For example, the plate scale will change if the upper DM has a static defocus. Calibration procedures must be applied to ensure that these errors do not compromise the astrometric performance of an MCAO system (e.g., flattening of the upper DM before closing the loop).

The limitations on astrometric accuracy imposed by the atmosphere are discussed in detail in TMT technical report #XX (Graham 2003)".

2.3.10 Radial Velocity

IFU with 20 or 35 mas slitlets/spaxels

The required radial velocity accuracy is 10 km/s which is a factor of 2 improvement over current observations with OSIRIS-LGSAO. Current accuracy is limited by:

1) Signal-to-noise:
   This will be improved by higher Strehl ratios.
2) Differential atmospheric refraction (chromatic):
   Should be compensated for by an infrared atmospheric dispersion corrector.
3) PSF estimation:
   Need to investigate how to improve PSF estimation for fields without good PSF stars.
4) Local background subtraction (diffuse Brγ gas over the entire field):
   Higher Strehls will yield sky estimates that are less contaminated by the halos of bright stars.
5) Spectral resolution (many lines are blends):
   Brγ (2.166 microns) and He (2.112 microns) lines are blends at R~4000. Higher spectral resolution would resolve the individual lines. Further investigation of the ideal spectral resolution is needed. In particular, if the NGAO system allows IFU spectroscopy of fainter stars, one may be able to obtain radial velocities from unblended spectral lines other than Brγ (2.166 microns) and He (2.112 microns).

2.3.11 Instrument requirements

Essential: High contrast near-IR imager with excellent astrometric performance (better than 0.1 mas).

Essential: Infrared integral field spectrometer, R ≥ 3000 that can achieve 10 km/sec radial velocity accuracy for stars near the Galactic Center.

Desirable but not absolutely essential: High resolution (R~15000) IFU spectroscopy. With this spectral resolution, radial velocity accuracies are improved to ~1 km/s and the radial velocity measurements may themselves constrain General Relativistic effects.

Imager:

Field of view:	at least 10 x10 arc sec
Field of regard:	IR tip-tilt stars available 1-20'' from imaging field center. Tip-tilt pickoff is required to be able to deal with multiple tip-tilt stars separated by only a few arcseconds.
IFU multiplicity:	one is sufficient
Wavelength coverage:	K-band

IFU Spectrometer:

Field of view:	at least 1 x 1 arc sec (more is desirable but not essential)

Field of regard: as needed to meet tip-tilt correction requirements
IFU multiplicity: one is sufficient
Wavelength coverage: K-band
Spectral resolution: (in addition, optional R~15,000)
Type and depth of required data pipeline: IFU pipeline for wavelength/flux calibration

2.3.12 References

Broderick, A. E., & Loeb, A. 2005, MNRAS, 363, 353

Diolaiti, E., 0. Bendinelli, D. Bonaccini et al. 2000, A&AS 147, 335

Eisenhauer, F., Schodel, R., Genzel, R., Ott, T., Tecza, M., Abuter, R., Eckart, A., & Alexander, T. 2003, ApJL, 597, L121

Genzel, R., Schodel, R., Ott, T., Eckart, A., Alexander, T., Lacombe, F., Rouan, D., & Aschenbach, B. 2003, Nature, 425, 934

Ghez, A. M., Salim, S., Hornstein, S. D., Tanner, A., Lu, J. R., Morris, M., Becklin, E. E., & Duchene, G. 2005, ApJ, 620, 744

Ghez, A. M., et al. 2004, ApJL, 601, L159

Ghez, A. M., et al. 2003, ApJL, 586, L127

Gondolo, P., & Silk, J. 1999, Physical Review Letters, 83, 1719

Miralda-Escude, J., & Gould, A. 2000, ApJ, 545, 847

Morris, M. 1993, ApJ, 408, 496

Olling, R. P., & Merrifield, M. R. 2000, MNRAS, 311, 361

Peebles, P. J. E. 1972, ApJ, 178, 371

Salim, S., & Gould, A.1999, ApJ, 523, 633

Schodel, R., Ott, T., Genzel, R., Eckart, A., Mouawad, N., & Alexander, T. 2003, ApJ, 596, 1015

Schodel, R., et al. 2002, Nature, 419, 694

Shen, Z.-Q., Lo, K. Y., Liang, M.-C., Ho, P. T. P., & Zhao, J.-H. 2005, Nature, 438, 62

Weinberg, N. N., Milosavljevic, M., & Ghez, A. M. 2005, ApJ, 622, 878

2.4 Galaxy Assembly and Star Formation History

Authors: D. Law. C. Steidel, J. Larkin
Editor: Claire Max

2.4.1 Introduction

Within the last decade the near infrared has become crucial for understanding the early universe and the evolution of galaxies. At redshifts above 1, galaxies have shrunk to angular sizes of approximately 1 arc sec making seeing based observations almost useless at uncovering morphologies and internal kinematics. At the epoch of greatest star formation and AGN activity around a redshift of 2.5, the traditional optical lines of Hα, OIII and OII are nicely shifted into the K, H and J bands respectively. The combination of the Keck LGS AO system with OSIRIS spatially resolved infrared spectroscopy is just now starting to dissect some of the brightest galaxies at this epoch. But with the factor of ~10 in sensitivity gain possible with Keck NGAO, a wealth of science topics can be addressed. These include the relationship between AGN and their host galaxies: radio galaxies and quasars have very strong emission lines and complex kinematics. In more "normal" galaxies, the redshift range from 1.5 to 2.5 is the key era for the birth of their first stars and the formation of the major architectural components, namely the bulge and disk. Measuring the morphology of star formation, the kinematics of proto-disks, the internal velocity dispersions and metallicity gradients (from things like the NII/Hα ratio) will allow us to witness the birth of galaxies like the Milky Way.

Table 4 gives a sample of which lines are available as a function of redshift.

Table 4

Redshift	J band	H band	K band
~ 1.2	Hα and NII		
~ 1.5	OIII	Hα and NII	
~ 2.5	OII	OIII	Hα and NII
~ 3.2		OII	OIII
~ 4.1			OII

Because JWST is optimized for faint-object IR spectroscopy and imaging, for this science case we will have to seek specific "sweet spots" in which Keck NGAO can make a significant contribution in the age of JWST.

Here we address science requirements flowing from one of these redshift ranges: $2 \le z \le 3$.

2.4.2 Scientific background and context: galaxies at $2 \le z \le 3$

At high redshifts z ~ 2-3 galaxies are thought to have accumulated the majority of their stellar mass (Dickinson et al. 2003), the rate of major galaxies mergers appears to peak (Conselice et al. 2003), and instantaneous star formation rates and stellar masses range over two decades in value (Erb et al. 2006). Given the major activity at these redshifts transforming irregular

galaxies into the familiar Hubble sequence of the local universe, it is of strong interest to study these galaxies in an attempt to understand the overall process of galaxy formation and the buildup of structure in the universe.

The global properties of these galaxies have recently received considerable attention, and the star formation rate, stellar mass, gaseous outflow properties, etc. have been studied in detail (e.g. Steidel et al. 2004, Papovich et al. 2006, Reddy et al. 2006 and references therein). Beyond these global properties however, little is known about their internal kinematics or small-scale structure, particularly with regard to their mode of dynamical support or distribution of star formation. Previous observations with slit-type spectrographs (e.g. Erb et al. 2004, Weiner et al. 2006) and seeing-limited integral field spectrographs (Flores et al. 2006) suggest that kinematics are frequently inconsistent with simple equilibrium disk models. However these studies are too severely constrained by slit misalignment, spatial resolution, and the size of the atmospheric seeing halo relative to the size of the typical sources (less than one arcsecond) to obtain conclusive evidence. It is therefore unknown whether the majority of star formation during this epoch is due to rapid nuclear starbursts driven by major merging of gas-rich protogalactic fragments, circumnuclear starbursts caused by bar-mode or other gravitational instabilities, or piecemeal consumption of gas reservoirs by overdense star forming regions in stable rotationally-supported structures.

Here we investigate the general capabilities of Keck NGAO for the study of these high-redshift galaxies, via simulations of the integral field spectrographs used to dissect these galaxies and to study their kinematics and chemical composition.

2.4.3 Scientific goals

The study of high-redshift galaxies is a powerful driver for multiplexed observations, for example via deployable integral field unit (IFU) spectrographs. Given the areal densities of 1 to 10 targets per square arcminute on the sky (depending on the target selection criteria, Table 5), multiplexing multi-conjugate or multi-object adaptive optics (MCAO/MOAO) systems would be capable of simultaneously observing ~ 10 targets within a several square arcminute field, permitting the compilation of a large representative sample with a minimum of observing time. In order to take best advantage of the high areal densities of targets, it is desirable to be able to deploy of order 6-12 IFUs over a ~ 5 square arcminute field of view.

Table 5

Space Densities of Various Categories of Extragalactic Targets.

Type of Object	Approx density per square arc minute	Reference
SCUBA sub-mm galaxies to 8 mJy	0.1	Scott et al. 2002
Old and red galaxies with $0.85 < z < 2.5$ and $R < 24.5$	2	Yamada et al. 2005; van Dokkum et al. 2006
Field galaxies w/ emission lines in JHK windows $0.8 < z < 2.6$ & $R < 25$	> 25	Steidel et al 2004; Coil et al 2004
Center of distant rich cluster of galaxies at $z > 0.8$	> 20	van Dokkum et al 2000
All galaxies $K < 23$	> 40	Minowa et al 2005

Such observations would permit the study of the chemical composition and distribution of star formation within the target galaxies (e.g. through mapping the measured [N II]/Hα ratios), in addition to mapping the velocity fields of the galaxies. Velocity data will enable us to detect AGN through chemical signatures and broadening of nuclear emission lines, to differentiate chaotic major mergers from starbursting galaxies in dynamical equilibrium, to determine the location of major star forming regions within any such rotationally supported systems, and to distinguish between chaotic and regular velocity fields to help ascertain whether observed star formation is commonly a consequence of major tidal interaction as predicted in current theories of galaxy formation.

With current-generation instruments, it is extremely challenging to observe a representative sample of sources due to the uncertainties inherent in long-slit spectroscopy (i.e. slit misalignment with kinematic axes), seeing-limited integral field spectroscopy (i.e. loss of information on scales smaller than the seeing disk), or a single-object IFU with current-generation adaptive optics (for which integration times are prohibitive for obtaining a large sample). A high-Strehl NGAO system with multi-object IFU capability would represent a major advance towards obtaining reliable kinematic and chemical data for a large sample of high redshift galaxies which could be productively integrated with the known global galaxy properties to further our understanding of galaxy formation in the early universe.

2.4.4 Proposed observations and targets

At redshifts z = 0.5-3, major rest-frame optical emission lines such as Hα, [N II], and [O III] fall in the observed frame near-IR, and in order to study the evolution of galaxies across this range of cosmic times it is important to have wavelength coverage extending from 1 to 2.5 microns. Hα line emission from the well-studied redshift $z \sim 2$-3 galaxy sample falls in the K band, emphasizing the importance of optimizing observations at these wavelengths by reducing backgrounds and inccreasing throughput as much as possible.

Typical observing strategy would entail simultaneous observation of approximately 10 high-redshift galaxies in a given field using a dithered set of exposures designed to move each object around on the detectors permitting maximum on-source integration time whilst simultaneously measuring accurate background statistics for sky subtraction. Based on the numerical simulations of Law et al. (2006) and the observed performance of the OSIRIS spectrograph, we anticipate that typical observations (assuming a K-band Strehl of roughly 60-70% from the NGAO system) would last approximately 1-2 hours per set of targets (for bright star-forming galaxies at redshift $z \sim 2$) permitting a sample of approximately 50 targets in a given night of dedicating observing.

2.4.5 AO and instrument requirements

2.4.5.1 AO requirements

Using the Gemini model of the Mauna Kea near-IR sky background coupled with a mathematical model of the thermal contributions from warm optical surfaces in the light path, Law et al. (2006) have demonstrated that the current K-band performance of AO-fed instruments is limited primarily by thermal emission from the warm AO system (which constitutes the majority of the total interline K band background). It is therefore a priority to reduce this emission to a lower fraction of the intrinsic background from the night sky and thermal radiation from the telescope itself. Using a combination of high-throughput optical components and AO system cooling, ideally we would like the thermal radiation from the AO system contribute less than 10-20% to the total K-band background. In Figure 6 we plot the AO cooling required (according to the Law et al. 2006 models) as a function of the throughput to achieve this goal.

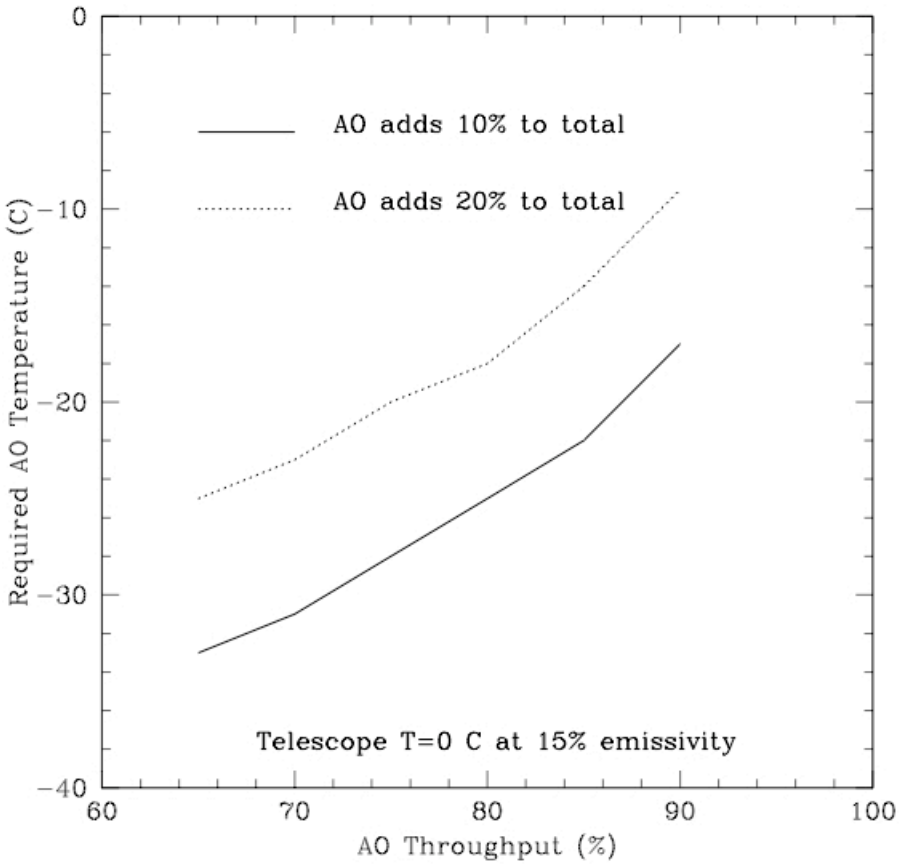

Figure 6 Required AO system temperature as a function of AO throughput to minimize impact of thermal radiation on the net K-band background.

Sky subtraction is key to obtaining quantitative spectral information. There are two ways to achieve this: 1) Given the typical size of the target galaxies (less than or of order an arcsecond), the field of view of each IFU could be suitably large to permit accurate sky subtraction (via on-IFU dithering) while sampling the target on the smallest scales permitted by detector noise characteristics. In this approach, each IFU should have a field of view measuring at least 3 x 1 arcseconds in order to avoid costly dedicated sky exposures. 2) The deployable integral field spectrgraph could include one or more arms that would be dedicated to taking spectra of the sky at the same time that galaxy spectra are being obtained on the other IFU arms. In this case each unit would only need to subtend 1 x 1 arcsecond on the sky. In the process of designing the deployable IFU spectrograph, there needs to be a trade study to evaluate and compare these two approaches to sky subtraction, as well as any other concepts that appear to be viable. It is not yet clear to us that option 2), using separate IFU heads in order to measure sky backgrounds, will yield accurate enough sky measurements.

The individual IFU units should be sampled on scales of order the diffraction limit (~ 50 mas) to permit accurate characterization of the structure on small scales without introducing excessive instrumental contribution to the total noise budget. Spectral resolution should be

greater than R~3000 in order to effectively resolve out OH sky features and distinguish Hα from [N II] emission.

Specifying AO requirements such as spatial resolution and encircled energy is not straightforward for the high-z galaxy science case. This is because the width of the core of the PSF will be limited by the availability of adequately bright tip-tilt stars. One can obtain excellent spatial resolution and encircled energy over that small fraction of the sky where excellent tip-tilt stars are available, or more modest spatial resolution and encircled energy over a larger fraction of the sky where tip-tilt stars are dimmer and/or farther away. AO requirements that deal with resolution alone are less useful than those that can be phrased in terms of "spatial resolution of xx achieved over a sky coverage fraction larger than yy". As we have not yet worked through this type of specification, we present the resolution and encircled energy requirements in terms of the desired IFU spaxel size, 50 mas.

AO Requirements:	**Near-IR**
Spaxel size (IFU spectroscopy)	50 mas
Field of view of one IFU unit	
Two options	1) 3 x 1 arc sec or greater (object size ~ 1", but need 3" in at least one dimension to get good sky meas't) 2) one or more dedicated IFU units for sky measurement. with each unit 1 x 1"
Backgrounds	Goal: < 10-20% above telescope + sky
Field of regard	As large as needed to get tip-tilt stars
Is a contiguous field required?	no
Encircled energy	50 mas with optimal tip-tilt stars
Sky coverage fraction	at least 30% with encircled energy radius < 75 mas
(Photometric accuracy)	
(Astrometric accuracy)	
(Polarimetry)	
(Contrast sensitivity)	

2.4.5.2 Instrument Requirements:

Field of view (spectroscopy)	3 x 1 arcsec or greater if sky subtraction is to be done within each IFU head. If there are separate IFU heads dedicated to sky subtraction, then field of view of 1 x 1 arcsec is adequate.
Field of regard	As large as needed for good tip-tilt
IFU or imager multiplicity	6-12
Wavelength coverage	JHK
Spectral resolution	3000 - 4000

Data reduction pipeline	Required
Other considerations	Atmospheric dispersion: may be able to avoid a dispersion corrector through appropriate data reduction pipeline software. The performance needs to be compared with that of a "real" ADC.

2.4.6 References

Coil, A. L. et al. 2004, ApJ, 617, 765

Conselice. C. et al. 2003, AJ, 126, 1183

Dickinson, M. et al. 2003, ApJ, 587, 25

Erb, D. K. et al. 2004, ApJ, 612, 122

Erb, D. K. et al. 2006, ApJ, 647, 128

Flores, H. et al. 2006, A&A, 455, 107

Law, D. et al. 2006, AJ, 131, 70

Minowa, Y. et al. 2005, ApJ, 629, 29

Papovich, C. et al. 2006, ApJ, 640, 92

Reddy et al. 2006, ApJ, 644, 792

Scott, S. E. et al. 2002, MNRAS, 331, 817

Steidel, C. C. et al. 2004, ApJ, 604, 534

van Dokkum, P. G. et al 2000, ApJ, 541, 95

van Dokkum, P. G. et al. 2006, ApJ, 638, L59

Weiner, B. J. et al. 2006, ApJ, 653, 1027 and ApJ, 653, 1049

Yamada et al. 2005

2.5 Roll-up of AO and Instrument Requirements

Table 4: AO Requirements Roll-Up

Science Case	Observing wavelengths	WFE	Enclosed Energy	Contrast	Sensitivity	Photometric accuracy	Astrometric accuracy	Radial velocity accuracy	Background	Polarimetric accuracy	Overheads between targets	Minimum sky coverage
Asteroid shape	0.7 – 2.4 μm	20% Strehl at R band	na	na		?	na	na	Equal to or lower than current LGS background	na	At most 10 min	?
Asteroid companions	0.7 – 2.4 μm	140 nm OK 170 and 200 nm under investigation	na	Δm = 5.5 at 0.5 arc sec sep'n		5% at 0.6 arc sec with Δm=3	Uncalibrated detector distortion < 1.5 mas	na	Equal to or lower than current LGS background	na	At most 10 min	?
Io												
Titan												
Planets around low-mass stars	0.9 – 2.4 μm plus possible L band	140 nm OK 170 and 200 nm under investigation	?	ΔH=13 at 1 arc sec sep'n	H=25 (5-sigma) in 20 minutes at 1˝arc sec sep'n	0.05 mag relative to primary star	~1/10 of the PSF FWHM	na	na	na	At most 10 min	> 30%
Protostellar objects												
Debris disks												
Galactic Center	K band (possibly L band)	170 nm at Gal. Ctr. (low elevation target)	?	High (not clear yet how high)			0.1 mas	10 km/sec	na (confusion limited)		na	Must give desired WFE at GC
Resolved Stellar Populations												
Nearby AGNs	0.8 - 2.4 μm	As low as possible	TBD	na			na	TBD			na	
QSO Host Galaxies												
Gravitational Lensing												
High z Galaxies	JHK bands		50% within 0.05 arc sec	na	Will depend on sky background		na		No more than 10-20% over sky plus telescope	na	na (long exposures)	> 30% with encircled energy of 75 mas

Keck NGAO: Instrument Suite Options
March 15, 2007

Key: **RED = primary instruments for each science case, BLUE = secondary instruments**

Science Case	NIR Imager Narrow Field Diffraction Limited	NIR IFU Narrow field R~4000 Diffraction Ltd	Vis Imager Narrow field Diffraction Limited	Vis IFU Narrow field Diffraction Limited	L+M band Imager Narrow field Diffraction Limited	NIR IFU Narrow field R~100 Diffraction Limited	NIR dIFU R~4000	NIR dImager	Vis dIFU	Vis dImager	R~15000 spectrometer or IFU	NIR differential polarimetry Narrow field Diffraction Limited
Asteroid shape	√ a few arc sec	√ a few arc sec	√a few arcsec	√ a few arc sec R~100								
Asteroid companions	√ a few arc sec	√ a few arc sec	√ a few arc sec	√ a few arc sec R~100								
Io	√ a few arc sec		√ maybe		√ a few arc sec							
Titan	√ a few arc sec	√ a few arc sec										
Planets around low-mass stars	√ 5 arc sec √ Coronagraph √ 0.9-2.4 micron				√ maybe	√ 5 arc sec √ Coronagraph? √ 0.9-2.4 micron						
Protostellar objects			√ a few arc sec									√ a few arc sec
Debris disks	√ a few arc sec √ What kind of coronagraph?		√ maybe									√ maybe
Galactic Center	√ 10 arc sec	√ 1 arc sec			√ maybe		√ yes				√ maybe	
Resolved Stellar Populations							√ maybe	√ >10 arc sec	√ maybe	√ >10 arc sec		
Nearby AGNs			√ with a long slit spectrograph capability (10-20 arc sec)	√ a few arc sec R~4000			√ maybe		√ yes			
QSO Host Galaxies	√ a few arc sec √ What kind of coronagraph?	√ a few arc sec	√ maybe									
Gravitational Lensing							√ a few arc sec	√ a few arc sec	√ maybe	√ maybe		
High z Galaxies	√ yes	√ yes					√ 1 x 3 arc sec or larger	√ a few arc sec				

3 Appendix A. Table of potential infrared tip-tilt stars close to the Galactic Center

Figure A1. Mosaic of Galactic Center at K band, from J. Lu and A. Ghez. The FITS file of this observation, which includes the WCS coordinate system, is available for use in correlating the image with the tables that follow.

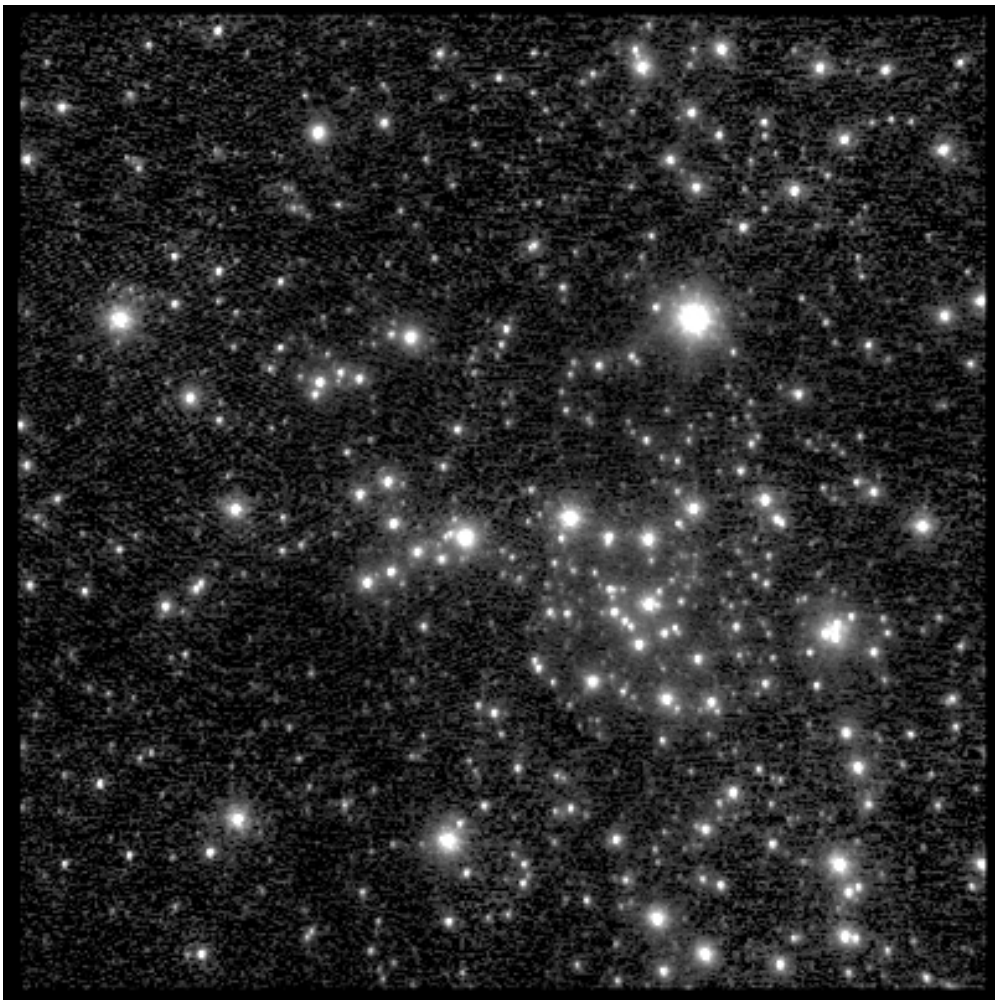

Following pages: Tables from Blum et al. 1996, ApJ 470, 864

TABLE 1

GALACTIC CENTER OBSERVED PHOTOMETRY

ID	Name	$\Delta\alpha$ (arcsec)[a]	$\Delta\delta$ (arcsec)[a]	K	$J-K$	$H-K$	$K-L$	Notes
1.....		−40.07	−8.01	10.40 ± 0.08	...	...	...	
2.....		−38.31	−22.60	10.27 ± 0.05	...	...	...	
3.....		−37.55	6.96	10.10 ± 0.05	...	...	...	
4.....		−34.38	−18.66	10.36 ± 0.04	6.85 ± 0.07	2.74 ± 0.06	...	
5.....		−29.36	−23.17	10.26 ± 0.03	6.61 ± 0.06	2.62 ± 0.05	...	
6.....		−28.49	−40.40	9.67 ± 0.03	...	...	...	
7.....		−26.91	18.90	9.80 ± 0.03	7.15 ± 0.06	2.76 ± 0.05	...	
8.....		−24.04	18.35	10.24 ± 0.06	6.65 ± 0.07	2.51 ± 0.07	...	
9.....		−23.04	16.43	9.92 ± 0.04	6.29 ± 0.05	2.42 ± 0.05	...	
10.....		−22.97	11.96	10.44 ± 0.04	7.11 ± 0.09	2.99 ± 0.05	...	
11.....		−22.40	41.86	9.22 ± 0.14	...	...	...	
12.....		−21.48	42.24	10.32 ± 0.08	5.34 ± 0.10	1.94 ± 0.11	...	
13.....		−20.12	−32.15	10.06 ± 0.03	7.42 ± 0.07	3.33 ± 0.05	...	H92
14.....		−19.30	25.37	10.48 ± 0.03	6.75 ± 0.05	2.68 ± 0.05	...	
15.....		−17.16	28.26	10.45 ± 0.03	6.27 ± 0.05	2.43 ± 0.05	...	H92
16.....		−16.97	10.34	9.59 ± 0.03	4.78 ± 0.04	1.70 ± 0.04	...	H92
17.....		−16.09	18.45	9.74 ± 0.03	6.07 ± 0.04	2.48 ± 0.05	...	
18.....		−13.72	15.34	10.18 ± 0.04	...	3.16 ± 0.05	...	
19.....		−13.27	−16.88	10.14 ± 0.03	7.57 ± 0.15	3.01 ± 0.05	...	H92
20.....		−10.90	−32.26	10.49 ± 0.04	...	2.52 ± 0.05	...	
21.....		−9.76	−25.81	10.24 ± 0.03	6.07 ± 0.05	2.24 ± 0.05	...	
22.....	BSD WC9	−9.69	−11.54	10.74 ± 0.05	...	2.08 ± 0.07	...	WC9
22.....	BSD WC9	−9.69	−11.54	10.72 ± 0.05	...	...	...	[b]
23.....		−9.59	6.47	9.75 ± 0.03	6.14 ± 0.04	2.31 ± 0.05	...	
24.....		−9.36	−17.17	10.18 ± 0.04	5.53 ± 0.05	2.05 ± 0.06	...	
25.....	AF NWB	−9.11	−8.97	11.67 ± 0.14	...	...	...	[b]
25.....	AF NWB	−9.11	−8.97	11.60 ± 0.09	5.26 ± 0.10	2.37 ± 0.12	...	
26.....	BSD WC9B	−9.08	−11.90	12.07 ± 0.13	...	...	...	[b]
26.....	BSD WC9B	−9.08	−11.90	12.04 ± 0.14	...	1.84 ± 0.18	...	
27.....		−9.05	−34.75	9.02 ± 0.03	...	2.66 ± 0.05	...	
28.....	IRS 11	−8.44	8.03	9.17 ± 0.07	5.95 ± 0.07	1.99 ± 0.08	...	Cool
29.....	AF NW	−8.24	−9.28	11.93 ± 0.17	...	...	...	[b]
29.....	AF NW	−8.24	−9.28	11.85 ± 0.11	5.15 ± 0.13	2.29 ± 0.15	...	He I
30.....	IRS 6WB	−8.17	−4.01	11.51 ± 0.42	...	...	...	[b]
31.....	IRS 6W	−8.12	−4.40	10.26 ± 0.14	...	...	...	[b]
31.....	IRS 6W	−8.12	−4.40	10.22 ± 0.05	5.78 ± 0.06	2.40 ± 0.07	...	
32.....	AF B	−7.79	−13.58	11.24 ± 0.07	5.25 ± 0.09	1.95 ± 0.09	...	
33.....	AF	−7.28	−12.89	10.74 ± 0.09	...	...	...	[b]
33.....	AF	−7.28	−12.89	10.70 ± 0.05	5.12 ± 0.06	2.06 ± 0.06	...	He I
34.....		−7.00	−27.69	10.19 ± 0.06	...	2.36 ± 0.07	...	[b]
35.....	IRS 30	−6.56	0.21	10.68 ± 0.08	...	...	...	
35.....	IRS 30	−6.56	0.21	10.49 ± 0.05	7.11 ± 0.16	2.49 ± 0.11	1.08 ± 0.23	[b]
36.....		−6.47	−22.39	10.37 ± 0.03	5.19 ± 0.04	1.85 ± 0.05	...	
37.....	IRS 30B	−5.87	−0.14	11.15 ± 0.16	...	...	...	
38.....	IRS 6E	−5.53	−5.08	10.06 ± 0.06	...	4.26 ± 0.17	...	WC9
38.....	IRS 6E	−5.53	−5.08	9.80 ± 0.06	...	...	2.96 ± 0.08	[b]
39.....		−5.03	−28.27	10.37 ± 0.04	6.20 ± 0.05	2.37 ± 0.05	...	
40.....		−4.89	−33.81	10.09 ± 0.05	...	...	...	
41.....		−4.50	−30.34	10.14 ± 0.09	...	2.39 ± 0.10	...	
42.....	IRS 13W	−4.45	−7.80	10.96 ± 0.12	...	...	...	Cool
42.....	IRS 13W	−4.45	−7.80	10.61 ± 0.11	...	...	2.87 ± 0.20	[b]
43.....		−4.29	−21.77	10.07 ± 0.03	6.13 ± 0.05	2.29 ± 0.05	...	
44.....	IRS 12NB	−4.16	−13.61	10.10 ± 0.10	5.69 ± 0.11	2.43 ± 0.12	...	
45.....	IRS 2	−4.15	−10.47	10.57 ± 0.06	...	3.65 ± 0.13	...	Cool
45.....	IRS 2	−4.15	−10.47	10.34 ± 0.09	...	...	2.29 ± 0.14	[b]
46.....	IRS 34	−4.13	−4.09	10.75 ± 0.07	...	...	...	He I
46.....	IRS 34	−4.13	−4.09	10.48 ± 0.08	...	2.83 ± 0.16	1.87 ± 0.19	[b]
47.....	IRS 12S	−4.10	−14.63	9.95 ± 0.05	5.85 ± 0.06	2.18 ± 0.06	...	Cool
48.....	IRS 22	−3.90	−31.98	8.03 ± 0.03	5.13 ± 0.04	1.77 ± 0.05	...	[c], Cool
49.....	IRS 2L	−3.87	−9.64	11.68 ± 0.20	...	...	4.37 ± 0.21	[d]
50.....	IRS 12N	−3.86	−12.91	8.58 ± 0.04	6.95 ± 0.05	2.83 ± 0.06	...	[c, e], Cool
50.....	IRS 12N	−3.86	−12.91	8.48 ± 0.05	8.68 ± 0.23	2.88 ± 0.06	0.80 ± 0.18	[b]
51.....		−3.51	−7.21	10.14 ± 0.20	...	...	...	
52.....	IRS 13E	−3.37	−7.51	9.82 ± 0.13	5.71 ± 0.14	2.34 ± 0.14	...	He I
52.....	IRS 13E	−3.37	−7.51	9.60 ± 0.15	...	...	3.21 ± 0.16	[b]
53.....	IRS 3	−2.45	−2.01	11.16 ± 0.11	...	...	...	Red
53.....	IRS 3	−2.45	−2.01	10.79 ± 0.07	...	...	5.52 ± 0.07	[b]
54.....	IRS A7	−2.10	2.71	10.50 ± 0.05	6.17 ± 0.06	2.42 ± 0.07	...	
55.....	IRS 29S	−1.93	−4.91	10.55 ± 0.28	5.90 ± 0.29	2.57 ± 0.29	...	Cool
56.....	IRS 29N	−1.79	−4.41	9.96 ± 0.11	...	...	...	WC9
56.....	IRS 29N	−1.79	−4.41	9.87 ± 0.11	...	...	2.67 ± 0.13	[b]
57.....	IRS 20	−1.45	−11.30	10.61 ± 0.05	5.89 ± 0.07	2.26 ± 0.07	...	Cool

TABLE 1—*Continued*

ID	Name	Δα (arcsec)[a]	Δδ (arcsec)[a]	*K*	*J*−*K*	*H*−*K*	*K*−*L*	Notes
57	IRS 20	−1.45	−11.30	10.56 ± 0.08	...	...	0.69 ± 0.49	[b]
58	F95 J	−1.33	11.60	10.38 ± 0.03	6.15 ± 0.05	2.40 ± 0.05	...	H92, Cool
59	MPE−1.0−3.5	−1.00	−3.76	11.90 ± 0.22	...	...	2.02 ± 0.46	[b], WC9
60	IRS 14SW	−0.73	−15.13	10.15 ± 0.04	6.72 ± 0.07	2.59 ± 0.06	...	Cool
61	IRS 33W	−0.68	−9.22	10.87 ± 0.07	6.07 ± 0.11	2.18 ± 0.10	...	Cool
61	IRS 33W	−0.68	−9.22	10.86 ± 0.11	...	...	1.01 ± 0.34	[b]
62	IRS 15SW	−0.43	5.95	10.39 ± 0.04	5.59 ± 0.05	2.15 ± 0.06	...	He I
63	IRS A11	−0.25	−8.07	10.92 ± 0.12	...	...	2.00 ± 0.18	[b]
63	IRS A11	−0.25	−8.07	10.87 ± 0.06	5.28 ± 0.07	2.05 ± 0.08	...	
64		−0.16	31.53	10.13 ± 0.03	6.53 ± 0.05	2.51 ± 0.05	...	
65	IRS 16NW	−0.08	−4.72	10.03 ± 0.07	...	...	...	[b], He I
65	IRS 16NW	−0.08	−4.72	10.03 ± 0.04	5.01 ± 0.06	2.01 ± 0.06	...	
66	IRS 7	0.15	−0.24	6.40 ± 0.03	6.64 ± 0.04	2.42 ± 0.10	...	[c, e], Cool
66	IRS 7	0.15	−0.24	6.70 ± 0.10	7.10 ± 0.14	2.60 ± 0.14	2.15 ± 0.14	[b]
67	IRS 33E	0.31	−9.13	10.02 ± 0.05	5.57 ± 0.06	2.21 ± 0.07	...	He I
67	IRS 33E	0.31	−9.13	9.86 ± 0.06	...	...	0.73 ± 0.25	[b]
68	IRS 14NE	0.36	−14.21	9.75 ± 0.04	6.80 ± 0.06	2.64 ± 0.06	...	Cool
69		0.39	−34.01	9.79 ± 0.03	7.02 ± 0.08	2.75 ± 0.05	...	
70	F95 B	0.44	−28.15	9.88 ± 0.06	6.30 ± 0.07	2.49 ± 0.08	...	Cool
71	IRS 16SW	0.67	−7.15	9.60 ± 0.05	5.15 ± 0.06	2.00 ± 0.07	...	He I
71	IRS 16SW	0.67	−7.15	9.34 ± 0.10	...	...	1.30 ± 0.12	[b]
72	F95 A	0.82	−36.34	9.05 ± 0.04	3.74 ± 0.05	1.27 ± 0.05	...	Cool
73		0.90	−7.70	10.03 ± 0.07	5.40 ± 0.08	2.05 ± 0.09	...	
74	IRS 16C	1.12	−5.61	9.86 ± 0.05	5.37 ± 0.06	2.13 ± 0.06	...	He I
74	IRS 16C	1.12	−5.61	9.79 ± 0.05	...	...	1.31 ± 0.09	[b]
75	IRS 15NE	1.38	5.61	8.96 ± 0.04	6.03 ± 0.05	2.41 ± 0.05	...	He I & Cool
76	OSUF 1	1.38	−12.49	11.40 ± 0.08	5.38 ± 0.11	2.18 ± 0.11	...	[f]
76	OSUF 1	1.38	−12.49	11.31 ± 0.14	...	...	...	[b]
77	MPE+1.6−6.8	1.58	−7.21	9.98 ± 0.06	6.00 ± 0.08	2.42 ± 0.08	...	WC9
77	MPE+1.6−6.8	1.58	−7.21	9.88 ± 0.14	...	...	2.00 ± 0.14	[b]
78	IRS 8	1.88	23.90	10.49 ± 0.06	...	...	...	Red
79		2.01	42.73	9.73 ± 0.13	6.60 ± 0.13	2.28 ± 0.13	...	
80	IRS 16CC	2.02	−5.61	10.51 ± 0.11	...	...	1.85 ± 0.16	[b]
80	IRS 16CC	2.02	−5.61	10.20 ± 0.07	5.36 ± 0.09	2.08 ± 0.09	...	He I
81	IRS 21	2.22	−8.83	10.40 ± 0.05	...	...	...	Red
81	IRS 21	2.22	−8.83	10.11 ± 0.06	...	...	3.20 ± 0.06	[b]
82	TAM He1	2.59	−11.82	12.05 ± 0.13	...	...	...	[g], He I
82	TAM He1	2.59	−11.82	12.01 ± 0.19	...	...	...	[b]
83	IRS 16NE	2.89	−4.90	9.01 ± 0.05	5.00 ± 0.06	1.93 ± 0.06	...	He I
83	IRS 16NE	2.89	−4.90	8.99 ± 0.05	...	...	1.44 ± 0.07	[b]
84		3.08	−17.50	9.88 ± 0.04	7.38 ± 0.08	3.06 ± 0.07	...	
85		3.12	−7.23	11.00 ± 0.08	5.08 ± 0.09	2.02 ± 0.10	...	
85		3.12	−7.23	10.95 ± 0.12	...	...	1.41 ± 0.20	[b]
86		3.45	−8.42	11.79 ± 0.13	...	...	...	
87	IRS A19	3.67	−13.25	11.61 ± 0.09	6.94 ± 0.29	...	1.85 ± 0.23	[b]
87	IRS A19	3.67	−13.25	11.18 ± 0.06	...	2.53 ± 0.08	...	
88		5.01	−13.32	10.03 ± 0.18	7.17 ± 0.20	...	...	
89	OSU He1	5.35	−3.01	12.36 ± 0.23	...	...	...	[f], He I
90		5.40	28.38	10.11 ± 0.08	5.82 ± 0.09	1.96 ± 0.09	...	
91	IRS 9	5.42	−12.60	8.53 ± 0.04	6.45 ± 0.05	2.46 ± 0.06	...	[c, e], Cool
91	IRS 9	5.42	−12.60	8.61 ± 0.03	7.33 ± 0.07	2.24 ± 0.04	1.45 ± 0.04	[b]
92	IRS 1W	5.42	−5.61	8.66 ± 0.04	...	...	3.16 ± 0.07	[b]
92	IRS 1W	5.42	−5.61	8.81 ± 0.04	6.21 ± 0.06	3.13 ± 0.07	...	[c], Red
93		6.63	−6.01	10.70 ± 0.13	5.86 ± 0.18	...	2.14 ± 0.22	[b]
93		6.63	−6.01	10.61 ± 0.13	...	2.37 ± 0.16	...	
94	IRS 10W	6.91	−0.97	10.27 ± 0.06	6.48 ± 0.08	3.13 ± 0.08	...	
94	IRS 10W	6.91	−0.97	10.22 ± 0.07	...	...	3.42 ± 0.07	[b]
95		7.07	−5.21	10.62 ± 0.09	6.04 ± 0.13	...	1.78 ± 0.17	[b]
95		7.07	−5.21	10.46 ± 0.07	...	2.56 ± 0.10	...	
96	IRS 1NE	7.28	−4.33	10.32 ± 0.08	...	...	1.50 ± 0.12	[b]
96	IRS 1NE	7.28	−4.33	10.00 ± 0.07	...	2.50 ± 0.09	...	Cool
97	IRS 1SE	7.49	−6.58	10.28 ± 0.06	...	...	...	[b]
97	IRS 1SE	7.49	−6.58	10.23 ± 0.04	6.66 ± 0.11	2.46 ± 0.06	...	Cool
98	IRS 10EL	8.07	−1.82	10.75 ± 0.09	...	...	4.25 ± 0.09	[d]
99		8.63	−24.83	9.76 ± 0.03	6.50 ± 0.05	2.45 ± 0.05	...	
100		8.80	3.79	10.38 ± 0.04	6.97 ± 0.08	3.92 ± 0.08	...	
101	IRS 10E	8.95	−2.04	10.36 ± 0.06	6.22 ± 0.07	2.17 ± 0.08	...	Cool
102	IRS 28	10.57	−12.09	9.36 ± 0.03	6.94 ± 0.05	2.81 ± 0.05	...	Cool
103	OSU C2	10.82	−5.03	10.10 ± 0.04	6.20 ± 0.06	2.35 ± 0.06	...	Cool
104		11.63	−2.42	10.47 ± 0.04	5.93 ± 0.05	2.21 ± 0.05	...	
105		13.32	−0.66	8.91 ± 0.03	6.28 ± 0.04	2.32 ± 0.05	...	
106		13.45	6.89	10.33 ± 0.03	6.27 ± 0.05	2.41 ± 0.05	...	

TABLE 1—*Continued*

ID	Name	Δα (arcsec)[a]	Δδ (arcsec)[a]	*K*	*J*−*K*	*H*−*K*	*K*−*L*	Notes
107.....		13.72	17.46	10.10 ± 0.03	6.27 ± 0.04	2.35 ± 0.04	...	
108.....	IRS 19	14.43	−25.74	8.22 ± 0.03	6.59 ± 0.04	2.61 ± 0.04	...	[e], Cool
109.....	IRS 18	14.94	−17.40	9.50 ± 0.03	6.36 ± 0.04	2.40 ± 0.04	...	
110.....		15.55	−28.56	10.07 ± 0.04	7.09 ± 0.07	2.95 ± 0.05	...	
111.....		16.55	44.67	10.39 ± 0.04	6.48 ± 0.10	2.24 ± 0.06	...	
112.....	OSU C3	17.09	−11.31	10.73 ± 0.04	...	3.06 ± 0.05	...	Cool
113.....		17.69	−0.87	10.01 ± 0.04	...	2.59 ± 0.07	...	
114.....		18.28	44.62	8.53 ± 0.04	5.81 ± 0.05	2.24 ± 0.05	...	[c]
115.....		20.23	22.67	10.26 ± 0.04	6.14 ± 0.05	2.35 ± 0.05	...	
116.....	OSU C1	20.61	−8.91	10.64 ± 0.04	...	2.53 ± 0.06	...	Cool
117.....		20.67	24.29	10.40 ± 0.04	5.90 ± 0.05	2.25 ± 0.05	...	
118.....		21.42	32.42	10.27 ± 0.03	6.04 ± 0.05	2.31 ± 0.04	...	
119.....		23.26	−25.08	10.38 ± 0.03	6.72 ± 0.06	2.59 ± 0.05	...	
120.....		23.31	−3.24	10.48 ± 0.03	7.00 ± 0.07	2.75 ± 0.05	...	
121.....		23.45	17.26	9.52 ± 0.03	7.13 ± 0.04	2.83 ± 0.04	...	
122.....		26.16	38.74	10.20 ± 0.04	5.67 ± 0.05	2.07 ± 0.05	...	
123.....		28.27	3.63	10.04 ± 0.03	6.88 ± 0.05	2.70 ± 0.04	...	
124.....		32.45	30.92	9.10 ± 0.03	5.34 ± 0.04	1.96 ± 0.04	...	
125.....		33.66	43.92	10.46 ± 0.04	6.39 ± 0.07	2.51 ± 0.06	...	
126.....		35.29	28.04	9.69 ± 0.03	6.86 ± 0.05	2.85 ± 0.05	...	
127.....		35.80	23.53	10.31 ± 0.08	4.91 ± 0.09	1.84 ± 0.10	...	
128.....	IRS 24	36.66	24.18	8.26 ± 0.04	6.36 ± 0.06	2.45 ± 0.05	...	[e], Cool
129.....		38.80	39.37	9.38 ± 0.03	5.47 ± 0.04	2.11 ± 0.05	...	
130.....		38.91	30.15	10.43 ± 0.03	6.10 ± 0.05	2.38 ± 0.05	...	
131.....		40.03	9.35	8.91 ± 0.03	5.31 ± 0.04	1.90 ± 0.05	...	
132.....		40.71	5.48	10.24 ± 0.03	6.23 ± 0.05	2.44 ± 0.05	...	
133.....		40.72	−29.72	9.20 ± 0.03	6.54 ± 0.04	2.63 ± 0.04	...	H92
134.....		40.74	−41.92	10.39 ± 0.03	4.80 ± 0.05	1.66 ± 0.05	...	
135.....	OSU C4	40.82	−4.50	10.67 ± 0.03	...	2.67 ± 0.04	...	Cool
136.....	IRS 23	42.51	8.19	8.62 ± 0.03	6.51 ± 0.04	2.58 ± 0.04	...	[e], Cool
137.....		43.67	40.36	10.18 ± 0.04	5.79 ± 0.05	2.17 ± 0.05	...	
138.....		45.68	11.15	10.40 ± 0.04	6.09 ± 0.05	2.65 ± 0.07	...	H92
139.....		46.08	0.38	9.89 ± 0.03	4.88 ± 0.04	1.75 ± 0.04	...	
140.....		46.84	15.82	9.44 ± 0.03	5.73 ± 0.04	2.16 ± 0.04	...	
141.....		48.27	22.84	10.23 ± 0.03	5.49 ± 0.04	2.01 ± 0.04	...	
142.....		53.16	25.96	9.91 ± 0.03	5.56 ± 0.04	2.14 ± 0.05	...	
143.....		56.84	28.00	9.86 ± 0.03	5.11 ± 0.04	1.88 ± 0.05	...	
144.....		56.93	18.83	10.30 ± 0.04	5.74 ± 0.05	2.15 ± 0.05	...	
145.....		62.56	22.02	10.45 ± 0.03	...	3.28 ± 0.05	...	
146.....		65.70	11.53	10.45 ± 0.03	7.24 ± 0.09	2.89 ± 0.05	...	H92
147.....		67.47	15.40	9.83 ± 0.04	4.63 ± 0.05	1.63 ± 0.05	...	

NOTES—All photometry is from our primary OSIRIS data set unless otherwise noted. The OSIRIS magnitudes include both measurement and calibration uncertainties. The DS91 data include only measurement uncertainty; calibration uncertainty is not included. IRS "A" names are taken from Tamura et al. 1996. Label "B" refers to a (usually) fainter source very close to the primary source. Earlier, lower resolution data likely included both components as a single source. H92 identifies a source of similar brightness and within 2″ of a variable star identified by Haller 1992. F95 refers to sources observed by Figer 1995. Cool identifies a star with CO 2.3 μm absorption based on *K*-band spectra; see LRT, Sellgren et al. 1987, Krabbe et al. 1995, and Paper II. He I identifies a star with 2.06 μm emission based on *K*-band spectra or narrow-band imaging; see Allen et al. 1990, Krabbe et al. 1991, 1995, Libonate et al. 1995, Blum et al. 1995a, and Tamblyn et al. 1996. Red identifies a star with a very red, nearly featureless spectrum based on *K*-band spectra; see Libonate et al. 1995, Blum et al. 1995a, and Krabbe et al. 1995. WC9 identifies a star with C III and C IV emission lines based on *K*-band spectra; see Blum et al. 1995b and Krabbe et al. 1995.

[a] Offset in arcseconds from IRS 7.

[b] Photometry derived from the DePoy & Sharp 1991 data set. *J* and *H* presented from DS91 data only if no value from the OSIRIS data was available (except for IRS 7, 9, and 12N; see note e below); see Appendix. The DS91 data were flux calibrated by assuming the IRS 7 magnitudes of Becklin et al. 1978 which are uncertain by less than ±0.1 mag at each wavelength. Good average agreement between the DS91 photometry and OSIRIS photometry argues that the assumed magnitudes of IRS 7 at the time of the DS91 observations were correct, despite the variability of IRS 7 (see text).

[c] *K* magnitude derived from narrow-band filters at 2.2 μm; see text.

[d] IRS 2 and 10E label the bright sources at *K*. IRS 2L and 10EL label the nearby, but not coincident, bright sources at *L*. For IRS 2L and 10EL we give *K* from OSIRIS and *L* from DS91. IRS 10EL has been identified as a variable star by Tamura et al. 1996 which they call IRS 10*. It may also be the OH/IR star OH 359.946−0.047 in the list of Lindqvist et al. 1992.

[e] See discussion in text on IRS 7, 9, and 12N variability. DS91 magnitudes for IRS 7 are from Becklin et al. 1978 as adopted by DS91. Uncertainty is less than ±0.1 mag at each wavelength. OSIRIS *H* magnitude for IRS 7 is from lower resolution image taken 2 months prior (1993 May 11) to the primary OSIRIS images; see text.

[f] OSU He1 (IRS A22) is an He I emission-line star; OSU F1 (IRS A15) is featureless, both based on unpublished *K*-band spectra.

[g] He I emission-line star identified by Tamblyn et al. 1996 narrow-band photometry, confirmed by our unpublished *K*-band spectrum.